Universal multifractal analysis as a tool to characterize multiscale intermittent patterns: example of phytoplankton distribution in turbulent coastal waters

Laurent Seuront[1], François Schmitt[2,5], Yvan Lagadeuc[1,6], Daniel Schertzer[3] and Shaun Lovejoy[4]

[1]*Station Marine de Wimereux, Université des Sciences et Technologies de Lille, CNRS-UPRESA 8013 ELICO, BP 80, 62930 Wimereux, France,* [2]*Institut Royal Météorologique, Section Climatologie Dynamique, 3 avenue Circulaire, 1180 Brussels, Belgium,* [3]*Laboratoire de Modélisation en Mécanique, Université Pierre et Marie Curie, CNRS-UMR 7607, Case 162, 4 place Jussieu, 75252 Paris Cedex 05, France and* [4]*Physics Department, McGill University, 3600 University Street, Montréal, H3A 2T8, Canada*

[5]*Present address: Department of Fluid Mechanics, VUB, Pleinlaan 2, 1050 Brussels, Belgium*

[6]*To whom correspondence should be addressed*

Abstract. A multifractal method of analysis, initially developed in the framework of turbulence and having had developments and applications in various geophysical domains (meteorology, hydrology, climate, remote sensing, environmental monitoring, seismicity, volcanology), has previously been demonstrated to be an efficient tool to analyse the intermittent fluctuations of physical or biological oceanographic data (Seuront *et al.*, *Geophys. Res. Lett.*, **23**, 3591–3594, 1996 and *Nonlin. Processes Geophys.*, **3**, 236–246, 1996). Thus, the aim of this paper is, first, to present the conceptual bases of multifractals and more precisely a stochastic multifractal framework which among different advantages lead in a rather straightforward manner to universal multifractals. We emphasize that contrary to basic analysis techniques such as power spectral analysis, universal multifractals allow the description of the whole statistics of a given field with only three basic parameters. Second, we provide a comprehensive detailed description of the analysis techniques applied in such a framework to marine ecologists and oceanographers; and third, we illustrate their applicability to an original time series of biological and related physical parameters. Our illustrative analyses were based on a 48 h high-frequency time series of *in vivo* fluorescence (i.e. estimate of phytoplankton biomass), simultaneously recorded with temperature and salinity in the tidally mixed coastal waters of the Eastern English Channel. Phytoplankton biomass, which surprisingly exhibits three distinct scaling regimes (i.e. a physical–biological–physical transition), was demonstrated to exhibit a very specific heterogeneous distribution, in the framework of universal multifractals, over smaller (<10 m) and larger (>500 m) scales dominated by different turbulent processes as over intermediate scales (10–500 m) obviously dominated by biological processes.

Introduction

Marine systems, globally dominated by turbulent events in coastal as in offshore locations (Grant *et al.*, 1962; Oakey and Elliott, 1982; Mitchell *et al.*, 1985), exhibit an intimate relationship between the structure of phytoplankton populations and their physical environment (Steele, 1974, 1976, 1978; Denman and Powell, 1984; Legendre and Demers, 1984). This association of physical and biological processes occurs over a whole range of scales, as shown by the patterns of physical, chemical and biotic parameters which are strongly interrelated within a given time period or spatial region (Cassie, 1959a,b, 1960). Even if for many decades many

investigators have shown that planktonic organisms are neither uniformly nor randomly distributed in the ocean (Hardy and Gunther, 1935; Cassie, 1963), these results are essentially related to spatial patterns associated with large- and coarse-scale physical processes (Mackas *et al.*, 1985). On the contrary, on fine and micro scales, which are of main interest for biological processes such as phytoplankton or zooplankton dynamics (Estrada *et al.*, 1987; Alcaraz *et al.*, 1988; Rothschild and Osborn, 1988; Sundby and Fossum, 1990; Thomas and Gibson, 1990; Granata and Dickey, 1991; Peters and Gross, 1994), very little is known about the effects of turbulent processes, basically regarded as a great factor of homogenization.

More specifically, physical processes, regarded as a main factor in structuring biological communities (Legendre and Demers, 1984; Mackas *et al.*, 1985; Daly and Smith, 1993), are intimately linked with the capability of organisms to aggregate (i.e. to create patches), at least in the case of phytoplankton communities. Plankton patchiness (variability at horizontal scales between 10 m and 100 km, and at vertical scales between 0.1 and 50 m; Mackas *et al.*, 1985) is then determined by the quasi-equilibrium which exists (or not) between biotic processes such as phytoplankton growth and hydrodynamism—basically estimated by the rate of kinetic energy ε—which was shown to be determinant in the size of patches which can maintain themselves in the face of diffusion (Skellam, 1951; Kierstead and Slobodkin, 1953; Denman and Platt, 1976; Wroblewski and O'Brien, 1976; Denman *et al.*, 1977; Okubo, 1978, 1980; Powell and Okubo, 1994) (e.g. the KISS length as defined by Okubo, 1980). Moreover, in addition to these theoretical investigations, the interactions between phytoplankton community dynamics and turbulent processes have been widely studied by numerous investigators (Platt *et al.*, 1970; Platt, 1972; Powell *et al.*, 1975; Denman, 1976; Fasham and Pugh, 1976; Steele and Henderson, 1977, 1992; Fortier *et al.*, 1978; Horwood, 1978; Lekan and Wilson, 1978; Demers *et al.*, 1979; Wiegand and Pond, 1979).

These pioneering approaches were essentially based on the assumption that turbulent processes can be regarded as homogeneous processes (Kolmogorov, 1941; Obukhov, 1941, 1949; Corrsin, 1951). However, it has been shown that not only turbulent fluid motions and the fluctuations of purely passive scalars such as temperature generate sharp fluctuations at all scales, but the distribution of these fluctuations, i.e. the activity of turbulence, is far from being homogeneous and rather extremely intermittent (Batchelor and Townsend, 1949; Kolmogorov, 1962; Obukhov, 1962). Thus, recent analysis conducted on zooplankton data (Pascual *et al.*, 1995), temperature and *in vivo* fluorescence (Seuront *et al.*, 1996a,b; Seuront, 1997) have shown that oceanic scalar fields were heterogeneously distributed over scales dominated by physical (i.e. turbulent) or biological processes.

Earlier statistical analysis techniques of plankton patchiness, such as models of point processes or power spectral analysis [see Fasham (1978) for a review] characterize variability in a very limited way. For instance, power spectral analysis, widely used in ecological applications (Platt and Denman, 1975), being only a second-order statistic, characterizes the variability very poorly by implicitly assuming 'quasi-Gaussian' statistics, which are not relevant for intermittent fields. For such fields, the best tool is provided by multifractal analysis, as shown by Pascual *et al.* (1995), Seuront *et al.* (1996a) and Seuront (1997) for planktonic fields.

Multifractals can be regarded as a rather considerable generalization of fractal geometry, essentially developed for the description of geometrical patterns (Mandelbrot, 1983). Indeed, fractal geometry has been introduced to describe the relationship—known as a scaling relationship—between patterns and the scale of measurement: the 'size' of a fractal set varies as the scale at which it is examined and raised to a (scaling) exponent, in this case given by the fractal dimension. The transition to the concept of multifractal fields (Grassberger, 1983; Hentschel and Procaccia, 1983; Schertzer and Lovejoy, 1983, 1985, 1987a; Lovejoy and Schertzer, 1985; Parisi and Frisch, 1985; Meneveau and Sreenivasan, 1987) leads to the consideration of multifractal fields as an infinite hierarchy of sets (loosely speaking, each of them corresponds to the fraction of the space where data exceed a given threshold) each with its own fractal dimension. Thus, multifractal fields are described by scaling relationships that require a family (even an infinity) of different exponents (or dimensions), rather than the single exponent of fractal patterns. Despite the apparent complexity induced by a multifractal framework, using the universal multifractal formalism (Schertzer and Lovejoy, 1987b, 1989), the distribution of a given scalar field can be wholly described by only three indices, which resume the statistical behaviour of turbulent fields from larger to smaller scales, as well as from extreme to mean behaviours.

Previous empirical and theoretical studies of phytoplankton patchiness (e.g. Platt, 1972; Denman and Platt, 1976; Denman *et al.*, 1977) have been able to quantify the scale of variation present in transects of chlorophyll, salinity and temperature, but have been able to say little about the precise variability associated with those scales. Herein, the goal of this paper is to provide to marine ecologists and oceanographers a detailed account of the universal multifractal techniques previously used for the description of phytoplankton biomass and temperature fluctuations (Seuront *et al.*, 1996a,b; Seuront, 1997) and their application to time series of *in vivo* fluorescence (i.e. phytoplankton biomass) and related physical parameters (i.e. temperature and salinity), taken from a fixed mooring in tidally mixed coastal waters of the Eastern English Channel. In that way, we provide an illustration of the applicability of these techniques in the characterization of the whole variability associated with specific scaling regimes identified with power spectral analysis: on small scales, where phytoplankton biomass distribution is controlled by turbulent processes, and at broader scales, where the variability in the biological and physical parameters such as cell growth and community structure, and horizontal processes, respectively, has an important role in shaping the phytoplankton distribution and overrides the local effects of turbulent mixing.

Background theoretical concepts in turbulence

Describing turbulent processes

Developed from 'intuitive' ideas (Richardson, 1922), a classical picture of turbulence treats it as a field of nested eddies of decreasing sizes, where turbulent kinetic energy 'cascades' with negligible dissipation from the largest energy-containing eddies to smaller and smaller eddies until it reaches Kolmogorov's length scale (i.e. viscous scale), where viscosity effects cannot be neglected and

start to smooth out turbulent fluctuations. Under the associated hypothesis of local isotropy and tri-dimensional homogeneity of turbulence, the velocity fluctuations of a given eddy can be described by the scaling relationships (Kolmogorov, 1941; Obukhov, 1949):

$$\Delta V_t \approx \varepsilon^{1/3} l^{1/3} \tag{1}$$

$$\Delta T_l \approx \varphi^{1/3} l^{1/3} \tag{2}$$

where $\Delta V_t = |V(x + l) - V(x)|$ and $\Delta T_l = |T(x + l) - T(x)|$ are the velocity and temperature shears at scale l, ε is the dissipation rate of turbulent kinetic energy and φ is the resulting flux of non-linear interactions of velocity and temperature fields given by $\varphi = \varepsilon^{-1/2} \chi^{3/2}$, where χ is the rate of temperature variance flux.

In Fourier space, the 1/3 law of velocity and temperature fluctuations in physical space [equations (1) and (2)] is associated with a power law for energy and variance power spectra (Figure 1) according to Obukhov (1941, 1949) and Corrsin (1951):

$$E_V(k) \approx \varepsilon^{2/3} k^{-5/3} \tag{3}$$

$$E_T(k) \approx \varphi^{2/3} k^{-5/3} \tag{4}$$

where k is a wavenumber.

However, contrary to the original proposal (Kolmogorov, 1941; Obukhov, 1941), it has been shown (Batchelor and Townsend, 1949; Kolmogorov, 1962; Obukhov, 1962) that the rate of energy flux ε and the rate of variance flux χ—respectively associated with velocity and temperature fluctuations—exhibit at all scales sharp fluctuations called intermittency (Figure 2). Turbulent velocity and temperature fluxes are intermittent in the sense that active regions occupy tiny fractions of the space available. Assumption of homogeneity is then untenable and turbulent fields have to be regarded as inhomogeneous and scale-dependent processes. Assuming the validity of the 'refined similarity hypothesis' (Kolmogorov, 1962; Obukhov, 1962), this leads to the introduction of the subscript l and to the modification of the relationships (1) and (2), respectively, as $\Delta V_t \approx \varepsilon_l^{1/3} l^{1/3}$ and $\Delta T_l \approx \varphi_l^{1/3} l^{1/3}$.

Modelling intermittent turbulence: from fractals to multifractals

Intermittent turbulence, fractal theory and multiplicative processes. Basically, the concept of eddies hierarchically organized in an isotropic cascade from large to small scales can be 'naturally' related to fractal properties in respect to the link existing between fractals and self-similarity (e.g. an object is called self-similar, or scale-invariant, if it can be written as a union of rescaled copies of itself, with the rescaling isotropic or uniform in all direction). However, the phenomenology of turbulent cascades is rather more complex than the expression 'eddy' would lead us to understand, since it becomes necessary to describe how the activity of
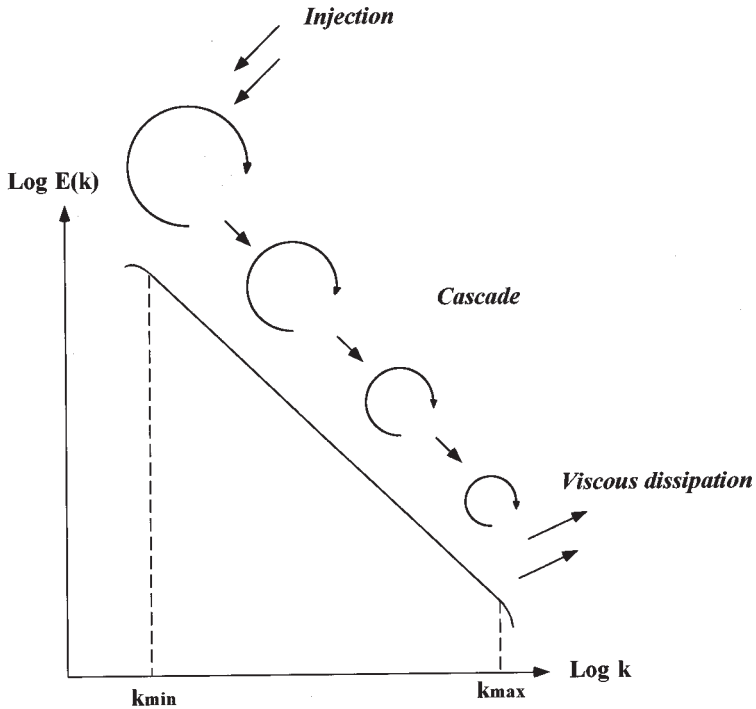
Fig. 1. Schematic representation showing the form of the frequency spectrum of turbulent velocity cascade, where $E(k)$ is the spectral density (variance units/$k)^2$ and k is a wavenumber (m^{-1}). The kinetic energy generated by large-scale processes (e.g. wind or tide) cascades through a hierarchy of eddies of decreasing size to the viscous subrange where it is dissipated into heat. The change in variance with wavenumber (i.e. slope of power spectrum) is scale invariant with a –5/3 slope as predicted by the theoretical Kolmogorov–Obukhov power law. The wavenumbers k_{max} and k_{min}, respectively, show the largest scale of creation of turbulence and the smallest scale (i.e. Kolmogorov length scale) reached by turbulent eddies where turbulent motions are smoothed out by viscous effects.

turbulence becomes more and more inhomogeneous at smaller and smaller scales. The simplest cascade model, the 'β-model' (Novikov and Stewart, 1964; Mandelbrot, 1974; Frisch *et al.*, 1978), takes the intermittent nature of turbulence into account by assuming that eddies are either 'dead' (inactive) or 'alive' (active). This cascade model has a discrete scale ratio between a parent structure and a daughter structure is introduced. For simplicity of implementation, this scale ratio is usually 2: one parent at scale l has 2 children at scale $l/2$. Using a notation including scale ratios $\lambda = L/l$ (where L is a fixed outer scale) associated to the scale l, we may write $\varepsilon_{2\lambda} = m.\varepsilon_\lambda$, where m is a multiplicative factor following the law:

$$\Pr(m = \frac{1}{\psi}) = \psi \qquad \text{'alive' sub-eddy} \qquad (5)$$

$$\Pr(m = 0) = 1 - \psi \qquad \text{'dead' sub-eddy} \qquad (6)$$

881
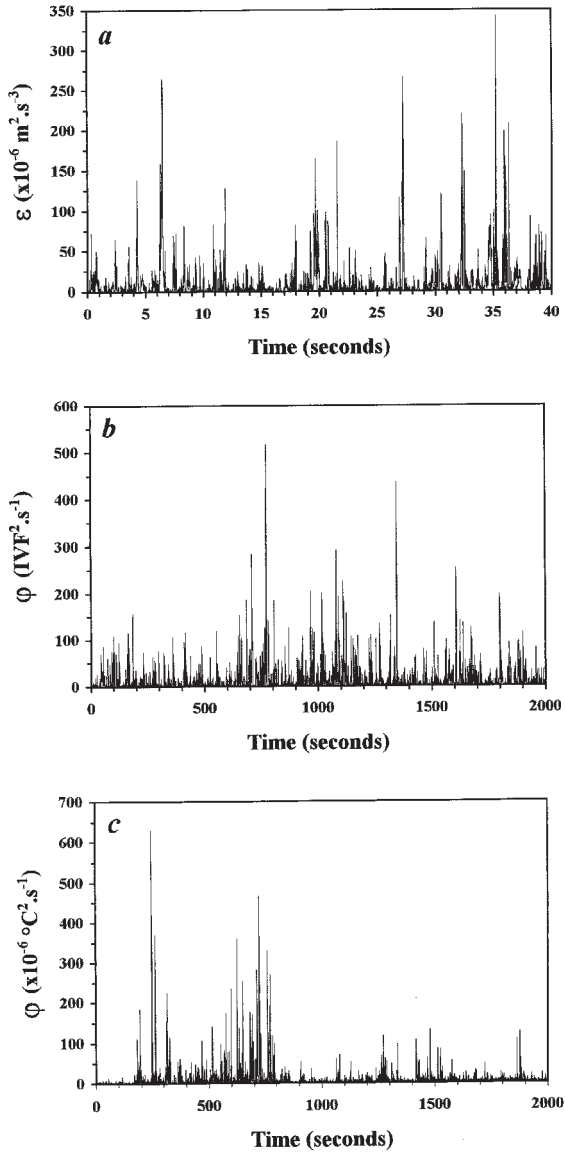
Fig. 2. Samples of the pattern of the rate of energy flux ε (**a**) estimated from grid generated turbulent velocity fluctuations recorded with a hot wire velocimeter, and the rates of variance fluxes φ estimated from *in vivo* fluorescence (**b**) and temperature (**c**) recorded in the Eastern English Channel with a Sea Tech fluorometer and a Sea-Bird 25 Sealogger CTD, respectively. Turbulent velocity, *in vivo* fluorescence and temperature fluxes exhibit at all scales sharp fluctuations called intermittency.

where ψ $(0 < \psi < 1)$ is the parameter of the model expressing the fraction of dead and alive eddies. This elementary process is then iterated n times until the total scale ratio $\lambda = 2^n$ is reached. If we denote $\psi = 2^{-c}$, then we have after n steps (if we take the first value $\varepsilon_1 = 1$):

$$Pr(\varepsilon_\lambda = \lambda^c) = \lambda^{-c} \qquad \text{'alive' sub-eddy} \qquad (7)$$

$$Pr(\varepsilon_\lambda = 0) = 1 - \lambda^{-c} \qquad \text{'dead' sub-eddy} \qquad (8)$$

In practice, this means that in an Euclidean space of dimension d, the 'β-model' (Figure 3) presents only λ^{-D} active sub-eddies, among λ^d potential sub-eddies (corresponding to the theoretical case of a homogeneous, or space-filling
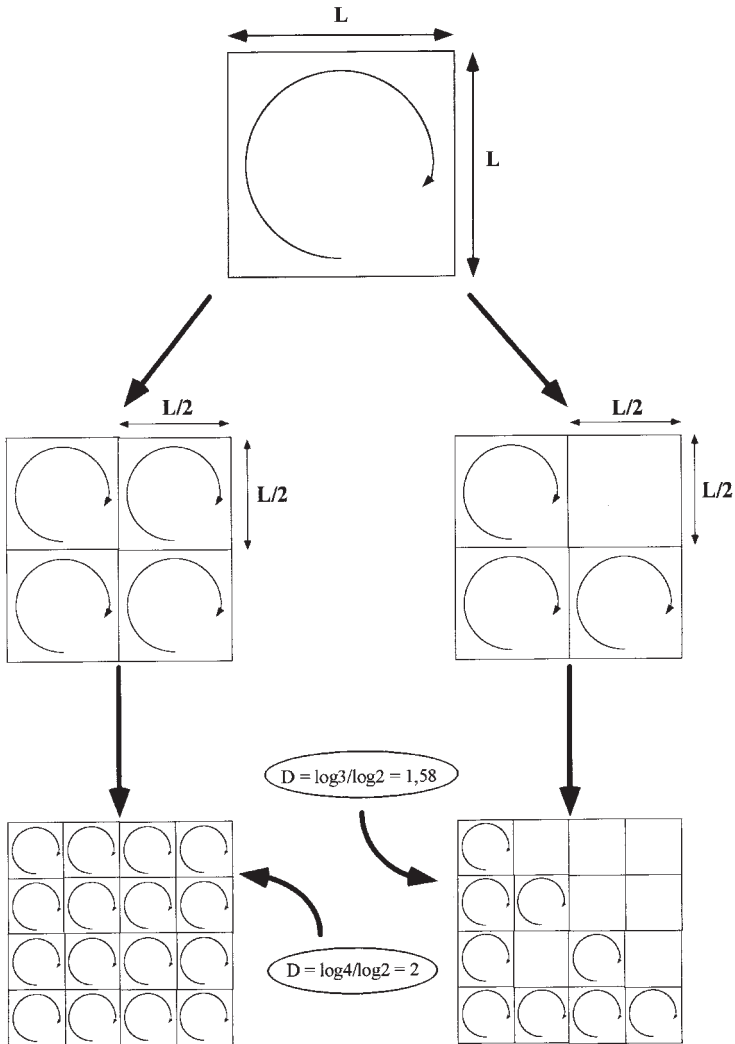
Fig. 3. Elementary isotropic cascades. The left-hand side shows a non-intermittent (i.e. homogeneous) cascade process corresponding to the hypothetical case of a space-filling turbulence. The right-hand side shows how intermittency can be modelled by assuming that not all sub-eddies are 'alive', leading to a (mono-) fractal description of turbulence. This is an implementation of the 'β-model' (adapted from Schertzer and Lovejoy, 1987b).

turbulence), c and D are, respectively, the fractal codimension and dimension characterizing the active eddies' activity, related as:

$$c = d - D \qquad (9)$$

where d is the dimension of the space considered ($d = 1$ for time series, $d = 2$ for bi-dimensional fields). It is already essential to note (Schertzer and Lovejoy, 1992) that c measures intrinsically the fraction of the space occupied by active eddies, i.e. its relative sparseness. Equation (9) corresponds merely to the fact that at each step of the cascade process, the fraction of space filled with alive eddies decreases by the factor λ^{-c} and conversely their energy flux density increases by the same factor to ensure average conservation.

The discrete 'β-model' is, however, only a caricatural approximation since it involves only dead and alive structures, an eddy is killed within a step of the cascade. It was indeed expected that the (mono-) fractal nature of this approximation was inadequate considering the realistic perturbations which correspond to replace the alternative dead or alive structures by the alternative weak or strong structures.

Discrete multiplicative cascades and multifractals. Rather than only allowing eddies to be either 'dead' or 'alive', the 'α-model' (Schertzer and Lovejoy, 1983, 1985) considers a more realistic feature allowing them to be either 'more active' or 'less active' (Figure 4). Equations (7) and (8) are then modified according to the following binomial process:

$$\Pr(\varepsilon_\lambda = \lambda^{\gamma^+}) = \lambda^{-c} \qquad \text{'strong' sub-eddy} \qquad (10)$$

$$\Pr(\varepsilon_\lambda = \lambda^{\gamma^-}) = 1 - \lambda^{-c} \qquad \text{'weak' sub-eddy} \qquad (11)$$

where γ^+ and γ^- ($\gamma^- < 0 < \gamma^+$) are, respectively, the strongest (with associated codimension c) and weakest singularities of the turbulent field, each singularity corresponding to an intermittency level. Figure 5 illustrates this mechanism for one step of the 'α-model' cascade. For n steps of the cascade process, the scale ratio between the largest eddy and the smallest one is then $\lambda = 2^n$ and the final pattern obtained (Figures 6 and 7) is very similar to the one observed in the case of turbulent field data (cf. Figure 2). With larger and larger number n of steps, more and more 'mixed' singularities γ ($\gamma^- < \gamma < \gamma^+$) are generated by the two initial 'pure' singularities γ^+ and γ^-. One may note here that the 'β-model' corresponds to the particular and peculiar case $\gamma^+ = c$ and $\gamma^- = -\infty$, which explains why contrary to the general case of the 'α-model', the iteration of the elementary step does not introduce new singularities and therefore yields a 'black and white' outcome.

When n becomes very large, intermittency can then be characterized by the statistical distribution of singularities γ ($\gamma^- < \gamma < \gamma^+$):

$$\varepsilon_\lambda \approx \lambda^\gamma \qquad (12)$$
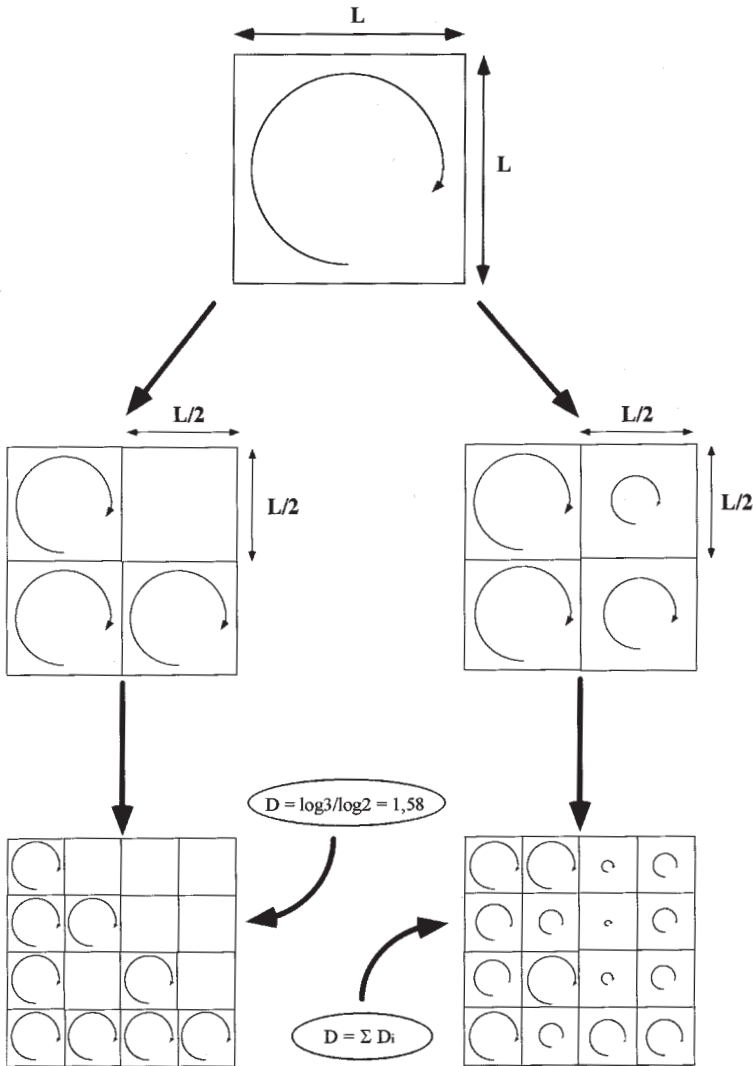
Fig. 4. These isotropic cascade processes show how the right-hand side multifractal 'α-model' generalizes the left-hand side monofractal 'β-model' by introducing a more realistic feature of intermittency. The 'α-model' allows eddies to be 'more active' or 'less active' rather than allowing them to be either 'dead' or 'alive', leading to a multifractal description of turbulence, each intermittency level being associated with its own fractal dimension.

and by the associated probability distribution (Schertzer and Lovejoy, 1987b):

$$Pr(\varepsilon_\lambda \geq \lambda^\gamma) \approx \lambda^{-c(\gamma)} \tag{13}$$

where $c(\gamma)$ is a function characterizing the singularities' distribution. One may note here that for a multifractal, the value of the field depends on the scale of
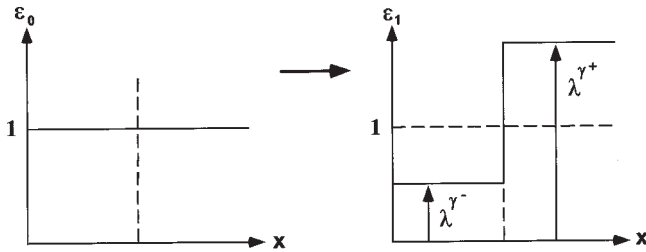
Fig. 5. Illustration of the 'α-model' for one step of cascade. The weak and strong sub-eddies have, respectively, an associated probability $Pr(\varepsilon_\lambda = \lambda^{\gamma-}) = 1 - \lambda^{-c}$ ($\lambda^{-c} < 0$) and $Pr(\varepsilon_\lambda = \lambda^{\gamma+}) = \lambda^{-c}$ ($\lambda^{-c} > 0$), rather than $Pr(\varepsilon_\lambda = 0) = 1 - \lambda^{-c}$ and $Pr(\varepsilon_\lambda = \lambda^c) = 1 - \lambda^{-c}$ expected in the case of inactive and active sub-eddies of the 'β-model'.
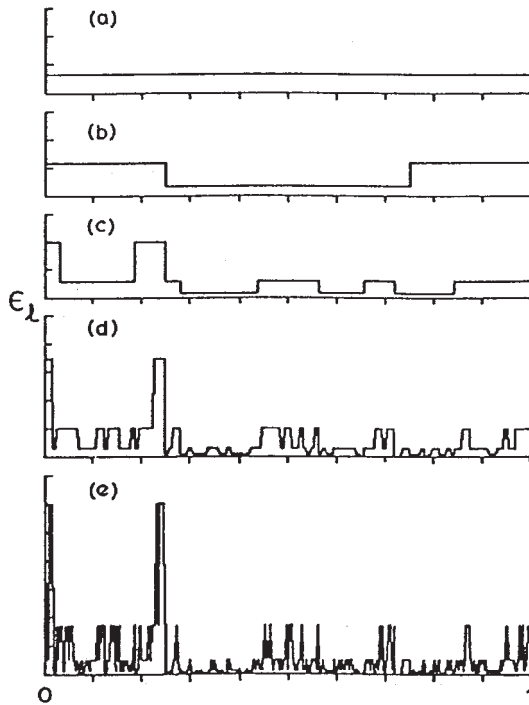
Fig. 6. A schematic representation of the 'α-model' generalizing Figure 5 for five steps of the cascade process. This shows a function which starts as homogeneous over the entire interval (**a**), whose scale of homogeneity is systematically reduced by a successive factor of 4 (**b**, **c**, **d** and **e**). Such a cascade model has the property of conserving the area under the curve (i.e. the energy flux to smaller scale), leading to a more and more sparse distribution of increasingly high peaks. The limit of the function when the scale of homogeneity goes to zero is dominated by singularities distributed over sparse fractal sets (redrawn from Schertzer and Lovejoy, 1987b).

observation, this is why λ is introduced here as a subscript. In practice, experimental data are recorded at the smallest available scale, and are then degraded through averaging, up to a given scale. As previously shown for *c* in the case of the monofractal 'β-model', $c(\gamma)$ is a codimension [for more discussion, see
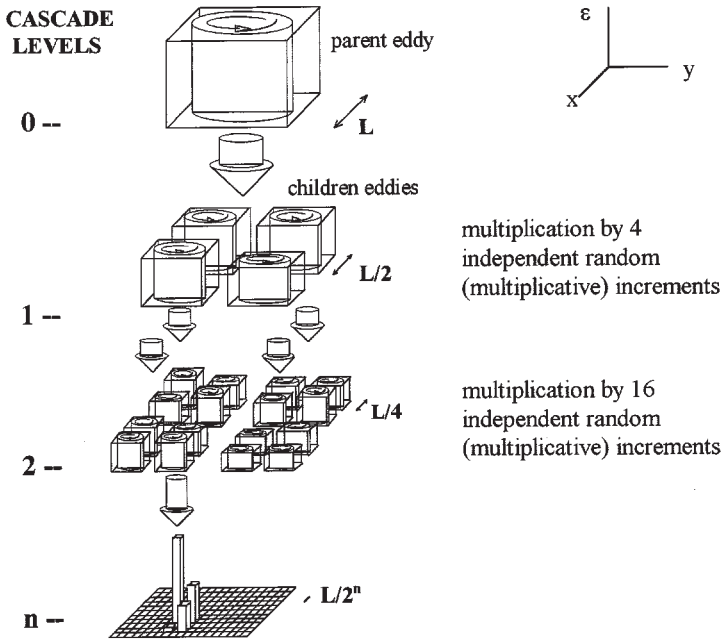
Fig. 7. A 2D schematic diagram showing a few steps of the discrete multiplicative cascade process of the 'α-model' with two orders of singularity γ^- and γ^+ (corresponding to the two values taken by the independent random increments $\gamma^{\gamma-} < 1$, and $\gamma^{\gamma+} > 1$), leading to the appearance of mixed orders of singularity γ ($\gamma^- \leq \gamma \leq \gamma^+$) (adapted from Schertzer et al., 1998).

Schertzer and Lovejoy (1992)]. Considering that among λ^d potential sub-eddies (i.e. in the case of a hypothetical space-filling turbulence) there are $\lambda^{-D(\gamma)}$ sub-eddies of different intensity, $c(\gamma)$ is expressed as a generalization of equation (9):

$$c(\gamma) = d - D(\gamma) \tag{14}$$

where $D(\gamma)$ characterizes the hierarchy of fractal dimensions associated with the different intermittency levels (i.e. singularities). That leads to consideration that the support of turbulence is defined by an infinite hierarchy of fractal dimensions rather than the single dimension of the 'β-model'. A turbulent process can then be regarded as a multifractal field, characterized by highly varying fractal dimensions in space and time in accordance with the local intensity of turbulent fluid motions.

Under fairly general conditions, the properties of the probability distribution of a random variable are equivalently specified by its statistical moments. The latter corresponds to the introduction of the scaling moment function $K(q)$ which describes the multiscaling of the statistical moments of order q of the turbulent field which writes:

$$\left\langle (\varepsilon_\lambda)^q \right\rangle \approx \lambda^{K(q)} \tag{15}$$

where '$\langle . \rangle$' indicates statistical or spatial averaging.

The relationship existing between the two scaling functions $c(\gamma)$ and $K(q)$ reduces to the Legendre transform (Parisi and Frisch, 1985) for large scale ratios (i.e. $\lambda \gg 1$):

$$K(q) = \max_\gamma \{q\gamma - c(\gamma)\} \Leftrightarrow c(\gamma) = \max_q \{q\gamma - K(q)\} \qquad (16)$$

Equation (16) implies that there is a one-to-one correspondence (see Figures 8 and 9 for an illustration) between singularities and orders of moments: to any order q is associated the singularity which maximizes $q\gamma - c(\gamma)$ and is the solution of $c'(\gamma_q) = q_\gamma$. Similarly to any singularity γ is associated the order of moment q_γ which maximizes $q\gamma - K(q)$ and is the solution of $K'(q_\gamma) = \gamma_q \cdot c(\gamma)$ and $K(q)$ exhibits several general properties of multifractals such as convexity and non-linearity. In particular, for conservative multifractal processes (i.e. $\langle\varepsilon_\lambda\rangle = \langle\varepsilon_1\rangle$, $\forall\lambda$) since $K(1) = 0$ corresponds via the Legendre transform to the fact that the corresponding mean singularity of the process, $C_1 = K'(1)$ is a fixed point of $c(\gamma)$, and by consequence the latter is tangential to the first bissectrix line $[c(\gamma) = \gamma]$ in $\gamma_1 = c(\gamma) = C_1$, hence $c'(C_1) = 1$. The determination of the probability distribution would require the determination of moments at all scales. With the assumption of scaling, it reduces to the determination of a hierarchy of exponents which remains nevertheless a priori infinite, and therefore indeterminable, especially for the highest orders which correspond to the most extreme variability. However, in the framework of universal multifractals (Schertzer and Lovejoy, 1987b, 1989, 1997; Lovejoy and Schertzer, 1990), the calculation complexity induced by the hierarchy previously described is included in few relevant exponents, which determine the moderate variability as well as the extreme variability.
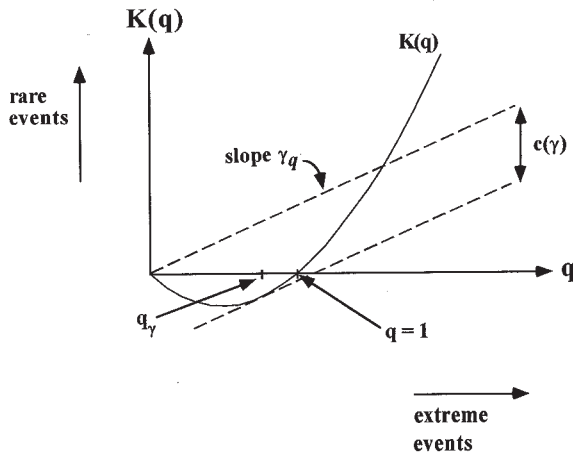
Fig. 8. $K(q)$ versus q showing the tangent line $K'(q_\gamma) = \gamma_q$. $K(q)$ exhibits several properties of multi-fractals such as convexity and non-linearity. One may note that the tangent line $K'(1) = C_1$ (not shown).
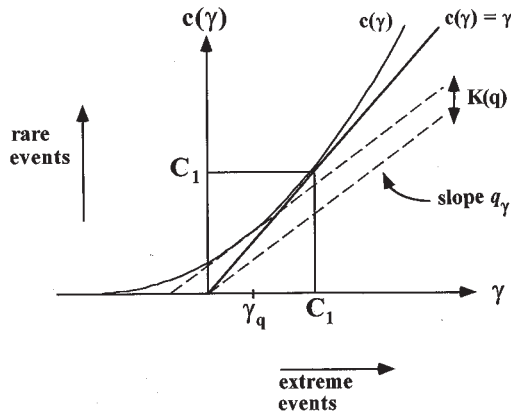
Fig. 9. $c(\gamma)$ versus γ showing the tangent line $c'(\gamma_q) = q_\gamma$. As $K(q)$, $c(\gamma)$ exhibits several properties of multifractals such as convexity and non-linearity. More precisely, $c(\gamma)$ is tangential to the first bissectrix line $[c(\gamma) = \gamma]$ in $\gamma_1 = c(\gamma_1) = C_1$.
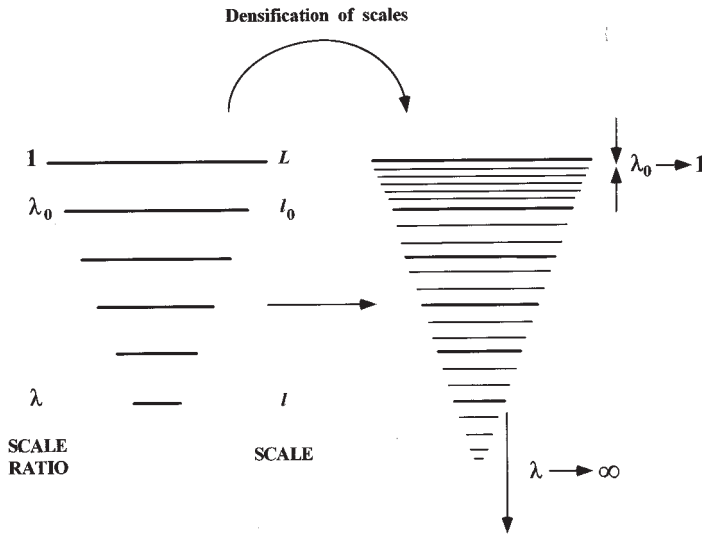
Continuous multiplicative cascades and universal multifractals. The discrete cascade processes discussed up to now to simulate intermittency are quite unrealistic because of the fixed scale ratio (usually) used at each step of the cascade. The continuous multiplicative cascade processes (Schertzer and Lovejoy, 1987b, 1989, 1997), developed as a way to view cascade phenomenology as a continuous process, are associated with a densification of scales which consist on the one hand of studying the limit $\lambda_0 \to 1$ adding more and more intermediate scales with a fixed global scale ratio $\lambda = \lambda_0^n$ and on the other hand the limit $\lambda \to \infty$ (Figure 10). However, as theoretically demonstrated (Schertzer and Lovejoy, 1987b, 1989, 1997; Lovejoy and Schertzer, 1990; Schertzer et al., 1991), the densification process converges on universal laws depending only on two fundamental parameters: C_1 and α, which describe the multiscaling behaviour of the scaling functions $K(q)$:

$$\begin{cases} K(q) = \dfrac{C_1}{\alpha - 1}(q^\alpha - q) & \alpha \neq 1 \\[2mm] K(q) = C_1 q \ln(q) & \alpha = 1 \end{cases} \tag{17}$$

and $c(\gamma)$:

$$\begin{cases} c(\gamma) = C_1 \left(\dfrac{\gamma}{C_1 \alpha'} + \dfrac{1}{\alpha} \right)^{\alpha'} & \alpha \neq 1 \\[2mm] c(\gamma) = C_1 \exp\left(\dfrac{\gamma}{C_1} - 1 \right) & \alpha = 1 \end{cases} \tag{18}$$

with $\dfrac{1}{\alpha} + \dfrac{1}{\alpha'} = 1$.

Densification of scales

Fig. 10. Scheme of the densification of scales process, leading to the viewing of cascade phenomenology as a continuous process. This densification consists both of studying the limit $\lambda_0 \to 1$ adding more and more intermediate scales and the limit $\lambda \to \infty$, where λ_0 and λ are, respectively, the smallest scale ratio (i.e. the ratio between two successive measurements) and the global scale ratio [i.e. the ratio between the fixed outer scale L and the smallest scale of measurement l ($\lambda = L/l$)].

C_1 is the mean singularity of the process, and also, as already pointed out above the codimension of the mean singularity, and therefore measures the mean fractality of the process. It satisfies $0 \leq C_1 \leq d$ (d is the Euclidean dimension of the observation space): $C_1 = 0$ for a homogeneous process and $C_1 = d$ for a process so heterogeneous that the fractal dimension of the set contributing to the mean is zero. It then characterizes a mean inhomogeneity and can be regarded as the measure of the sparseness of a given field: the higher the C_1, the fewer the field values corresponding to any given singularity (Figure 11a). The index α, called the Lévy index, is the degree of multifractality bounded between $\alpha = 0$ and $\alpha = 2$ which correspond, respectively, to the monofractal 'β-model' and to the log–normal model. It defines how fast the fractality is increasing with higher and higher singularities: as α decreases, the high values of the field do not dominate as much as for larger values of α; there are more large deviations from the mean (Figure 11b).

It can be noticed here that the whole previous developments, conducted in the framework of turbulence, can be applied to a great variety of intermittent fields. Indeed, they do not depend on the fact that the governing equations are known or not: when these equations are known (e.g. in the framework of turbulence), one uses until now only their scaling symmetry, not the other ones [see Schertzer *et al.* (1998) for discussion on new alternatives to bridge this gap between phenomenology and governing equations]. This is the main reason that the following class of multifractal models, often called Fractionally Integrated Flux
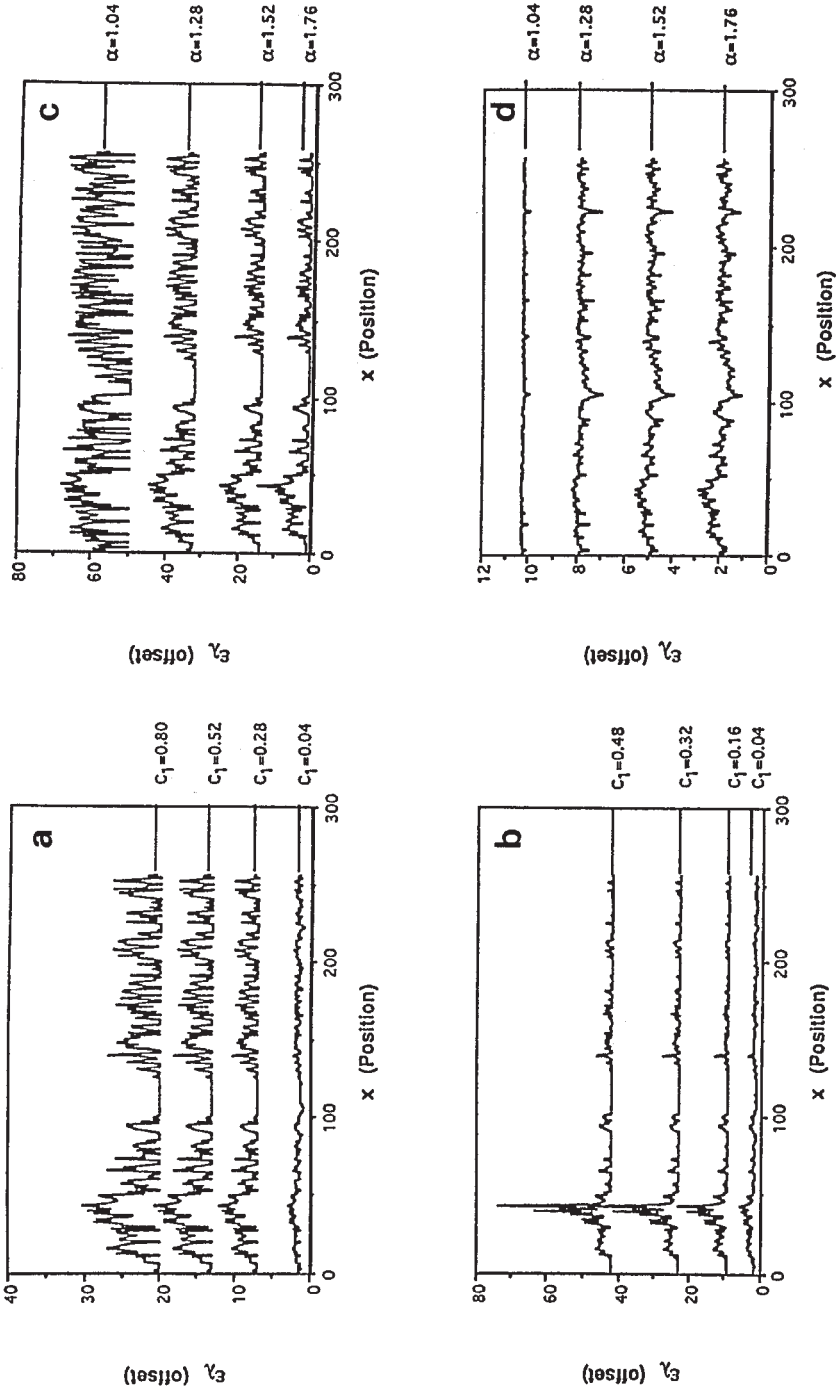
Fig. 11. Illustration of turbulent field ε_λ (i.e. the turbulent kinetic energy dissipation rate) properties described by the universal multifractal parameters C_1 and α using one-dimensional simulations of length 256, with $C_1 = 0.9$ (**a**) and $C_1 = 0.001$ (**b**) and varying α, and with $\alpha = 1.4$ (**c**) and $\alpha = 2.0$ (**d**) and varying C_1. These simulations have been vertically offset so as not to overlap (redrawn from Pecknold *et al.*, 1993).

models (FIF), became used in geophysical fields not related directly to turbulence: in analogy with turbulence, a flux ϕ_l, usually associated to some invariance or conservative property, is defined from a given intermittent scalar field S with a scaling relationship similar to those relating flux of energy ε and velocity shears, or flux φ and temperature gradients [equations (1) and (2)]:

$$\Delta S_l \approx \phi_l^a l^H \tag{19}$$

where H $(0 \leq H \leq 1)$ is a parameter which characterizes in a general manner (and in a very precise manner when $a = 1$) the degree of non-conservation of the field ($H = 1/3$ for a scalar quantity passively advected by non-intermittent turbulence), whereas the power of the flux is often taken as $a = 1$ for simplicity (Schertzer and Lovejoy, 1987b; Teissier *et al.*, 1993a,b). However, the most important meaning of H corresponds to the fact that it is the order of fractional differentiation in order to obtain the flux ϕ_l from the field S [see Schertzer *et al.* (1998) for more discussion (in particular for space–time FIF models) and further details]. Let us mention briefly that an isotropic fractional differentiation corresponds to a multiplication by k^H in Fourier space equivalent to power law filtering.

Data analysis techniques

Spectral analysis. Basically applied to a variety of geophysical and ecological data (Platt and Denman, 1975; McHardy and Czerny, 1987; Ladoy *et al.*, 1991; Olsson *et al.*, 1993) to detect scaling behaviours, spectral analysis corresponds to an analysis of variance in which the total variance of a given process is partitioned into contributions arising from processes with different length scales or time scales in the case of spatially or temporally recorded data, respectively. A power spectrum separates and measures the amount of variability occurring in different wavenumber or frequency bands. When all or parts of the spectrum follow a power law like equations (3) and (4), i.e. $E(k) \approx k^{-\beta}$, the data are scaling in that range, i.e. the scaling regime. β is the exponent characterizing spectral scale invariance: for instance $\beta = 5/3$ in homogeneous turbulence. The absence of characteristic time scales and the presence of a scaling regime indicate that a multifractal analysis may prove to be successful.

Structure functions. A power spectrum being a second-order moment, it rather characterizes a mean variability, i.e. a mean scaling behaviour. Then, the previous spectral analysis is generalized with the help of the qth-order structure functions (Monin and Yaglom, 1975):

$$\left\langle (\Delta S_\tau)^q \right\rangle = \left\langle |S(t + \tau) - S(\tau)|^q \right\rangle \tag{20}$$

where for a given time lag τ the fluctuations of the scalar S are averaged over all the available values ('<.>' indicates statistical averaging). For scaling processes, one way (Monin and Yaglom, 1975; Anselmet *et al.*, 1984) to characterize intermittency statistically is based on the study of the scale invariant structure exponent $\zeta(q)$ defined by:

$$\left\langle (\Delta S_\tau)^q \right\rangle = \left\langle (\Delta S_T)^q \right\rangle \left(\frac{\tau}{T} \right)^{\zeta(q)} \tag{21}$$

where T is the largest period (external scale) of the scaling regime. The scaling exponent $\zeta(q)$ is estimated by the slope of the linear trends of $\langle (\Delta S_\tau)^q \rangle$ versus τ in a log–log plot. The first moment, characterizing the scaling of the average absolute fluctuations, corresponds to the scaling 'Hurst' exponent $H = \zeta(1)$, previously introduced in equation (19) to characterize the degree of non-conservation of a given field. The second moment is linked to the power scaling exponent β by $\beta = 1 + \zeta(2)$. For simple (monofractal) processes, the scaling exponent of the structure function $\zeta(q)$ is linear: $\zeta(q) = qH$ [$\zeta(q) = q/2$ for Brownian motion and $\zeta(q) = q/3$ for Obukhov–Corrsin non-intermittent turbulence]. For multifractal processes, this exponent is non-linear and concave.

Moreover, multifractal processes possessing stable and attractive generators (Schertzer and Lovejoy, 1987b, 1989; Schertzer *et al.*, 1995), in the universal multifractals framework, the departure from linearity of the scale invariant structure function exponent $\zeta(q)$ is then given by the universal multifractal parameters α and C_1:

$$\zeta(q) = qH - \frac{C_1}{\alpha - 1}(q^\alpha - q) \tag{22}$$

with $K(q) = \dfrac{C_1}{\alpha - 1}(q^\alpha - q)$ [see equation (17)]. The parameter H is the degree of non-conservation of the average field [$\zeta(1) = H$]: $H = 0$ and $H \neq 0$ mean that the fluctuations are, respectively, scale independent and scale dependent [H ranges from 0.34 to 0.42, and 0.36 to 0.43, respectively, for temperature and passive *in vivo* fluorescence, see Seuront *et al.* (1996a,b), Seuront (1997); and $H \approx 0.12$ for fluorescence over scales dominated by biological activity, see Seuront *et al.* (1996a)]. The second term expresses a deviation from homogeneity [in which case $\zeta(q) = qH$], and represents the intermittency effects.

Double Trace Moment. The Double Trace Moment analysis technique (Lavallée, 1991; Lavallée *et al.*, 1992) is a generalization of the expression given by equations (15) and (17) to a quantity $(\phi_\Lambda)^\eta$ by taking the ηth power of the field ϕ_Λ—which is the general field Φ_l defined by equation (19) at the scale ratio Λ— and then studying its scaling behaviour at decreasing value of the scale ratio $\lambda \leq \Lambda$. Hence, the new generated field has the following multiscaling behaviour:

$$\left\langle \left[\phi_{\lambda,\Lambda}^\eta \right]^q \right\rangle \approx \lambda^{K(q,\eta)} \tag{23}$$

where $K(q,\eta)$ is the double trace moment scaling exponent related to $K(q,1) \equiv K(1)$ by:

$$K(q,\eta) = K(q\eta) - qK(\eta) \tag{24}$$

which gives for universality classes [using equation (17)]:

$$K(q,\eta) = \eta^\alpha K(q) \tag{25}$$

The scaling exponent $K(q,\eta)$ is estimated by the slope of the linear trends of $\left\langle \left[\phi^\eta_{\lambda,\Lambda} \right]^q \right\rangle$ versus λ in a log–log plot. By keeping q fixed (but different from the special values 0 and 1), the slope of $|K(q,\eta)|$ as a function of η in a log–log graph gives the value of the index α and C_1 is estimated by the intersection with the line $\eta = 1$. Varying then allows a systematic verification of equation (25), and hence the universality hypothesis.

Case study: tidally turbulent coastal waters of the Eastern English Channel

Data sampling

Sampling experiments were conducted during 46 h and 24 min in a period of spring tide, from 2 to 4 April 1996, at an anchor station (Figure 12) located in inshore waters of the Eastern English Channel (50°47′300 N, 1°33′500 E). Temperature and salinity, regarded as passive scalars under purely physical control of turbulent motions, and phytoplankton biomass, estimated from measurements of *in vivo* fluorescence intensity, were simultaneously recorded from a single depth (10 m) with Sea-Bird 25 Sealogger CTD probe and a Sea Tech fluorometer, respectively. Our analyses are based on three time series recorded at 1 Hz (i.e. 167 040 data), which contain temperature, salinity and fluorescence data, labelled A, B and C, respectively. Samples of these data are shown in Figure 13. Every hour, samples of water were taken at 10 m depth to estimate chlorophyll *a* concentrations, which appear significantly correlated with *in vivo* fluorescence (Kendall's $\tau = 0.652$, $P < 0.05$).

*Scaling and multiscaling of temperature, salinity and fluorescence fields*

Power spectral analysis. We compute the Fourier power spectra of temperature, salinity and *in vivo* fluorescence fluctuations in order to estimate the mean scaling properties of those different fields (Figure 14). The temperature and salinity power spectra exhibit very similar scaling behaviours [i.e. $E(f) \propto f^\beta$, where f is the frequency] over the whole range of studied scales (Figure 14a and b). Over smaller scales (1–1000 s), the observed power law trend gives $\beta \approx 1.72$ and $\beta \approx 1.67$ for temperature and salinity, respectively. Over larger scales (>1000 s), temperature and salinity power spectra both exhibit steeper power law trends with $\beta \approx 1.98$ and $\beta \approx 2.25$, respectively. The fluorescence power spectrum (Figure 14c) presents a slightly complex behaviour with three scaling tendencies for scales ranging from 1 to 20 s with $\beta \approx 1.77$, from 20 to 1000 s with $\beta \approx 0.66$ and for scales larger than 1000 s with $\beta \approx 1.96$. Those temporal transitional scales can be associated with spatial scales using probably the most cited and widely used method of relating time and space, 'Taylor's hypothesis of frozen turbulence' (Taylor, 1938), which basically states that temporal and spatial averages t and l,
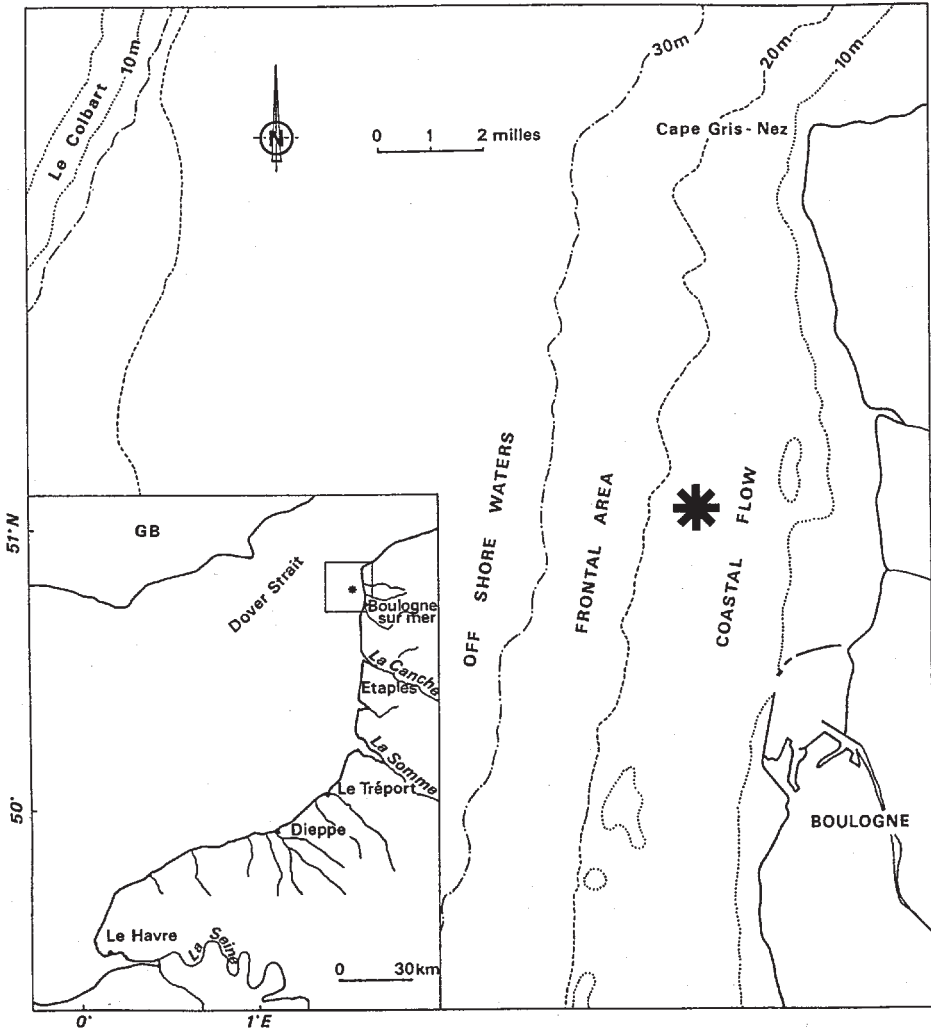
Fig. 12. Study area and location of the sampling station (*) along the French coast of the Eastern English Channel.

respectively, can be related by a constant velocity V, $l = V \cdot t$. Then, using the mean instantaneous tidal circulation of ~0.541 m s^{-1} (0.541 ± 0.126 SE), observed during the field experiment, the associated transitional length scales are around 12 and 540 m for *in vivo* fluorescence, and 540 m for temperature and salinity.

At small scales, the relative proximity between the spectral behaviour of temperature, salinity and fluorescence seems to confirm the hypothesis of passivity of phytoplankton biomass in a turbulent environment. Indeed, the departure from the expected theoretical value ($\beta \approx 5/3$) associated with the behaviour of a passive scalar in fully developed turbulence (Obukhov, 1949; Corrsin, 1951) is not
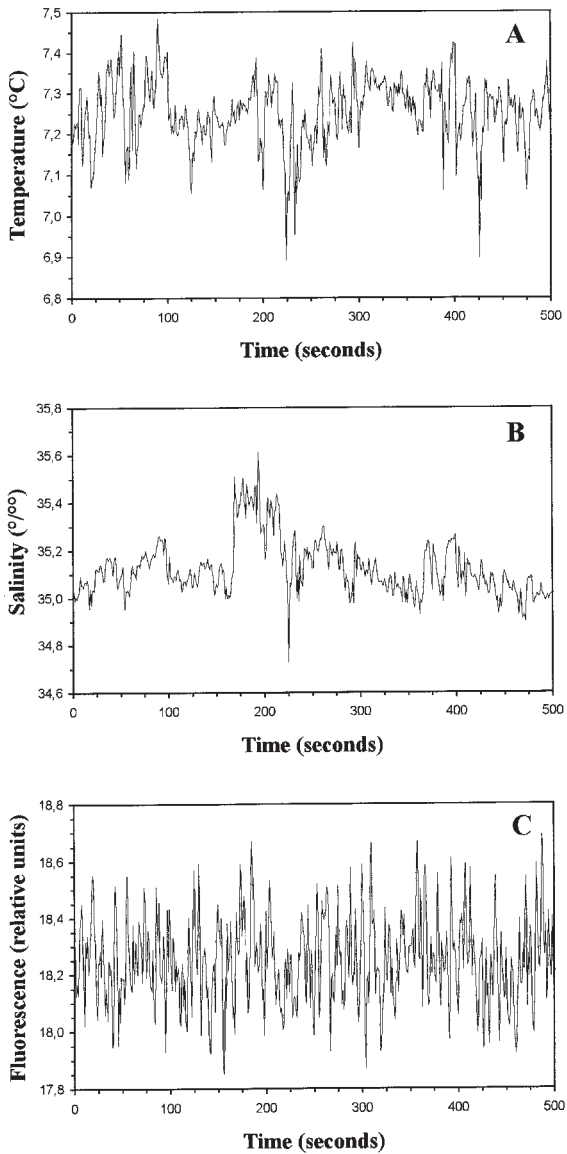
Fig. 13. A portion of temperature, salinity and *in vivo* fluorescence time series (from top to bottom) recorded in the Eastern English Channel. Sharp fluctuations occurring on all time scales are clearly visible, indicating the intermittent behaviour of the dataset.

significant (modified *t*-test, $P < 0.05$; Scherrer, 1984). These results, in agreement with previous field studies showing chlorophyll spectra which follow approximately the –5/3 power law (e.g. Platt, 1972; Powell *et al.*, 1975), seem to indicate that, over these small scales, the space–time structure of phytoplankton biomass is primarily influenced by the dynamics of the physical environment, rather than
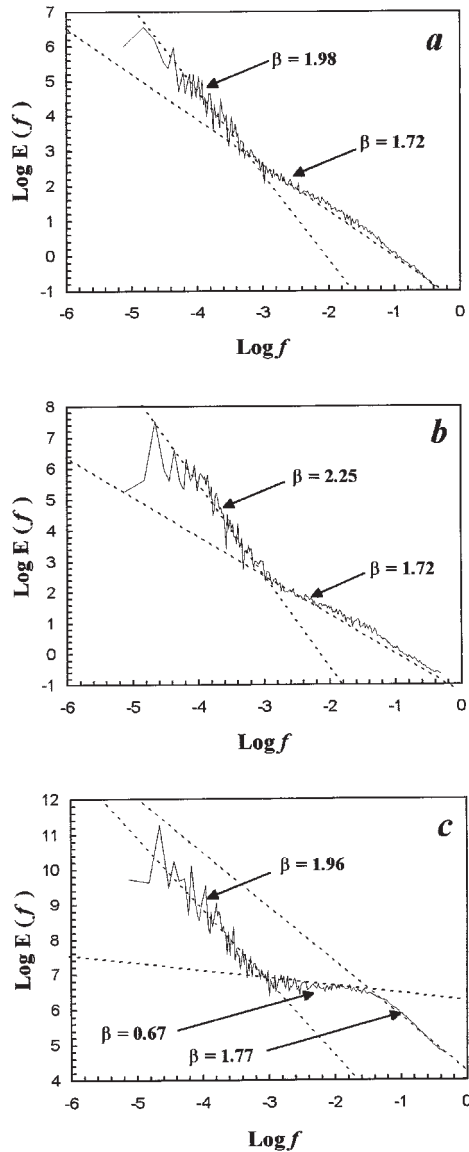
Fig. 14. The power spectra $E(f)$ (f is frequency) of temperature (**a**), salinity (**b**) and *in vivo* fluorescence (**c**), shown in log–log plots. Temperature and salinity power spectra exhibit two similar scaling regimes for scales ranging from 1 to 1000 s and for scales >1000 s, whereas *in vivo* fluorescence power spectrum exhibits a more complex behaviour with three scaling regimes for scales ranging from 1 to 20 s, 20 to 1000 s and for scales >1000 s.

the behaviour of the organisms themselves. On the other hand, over larger scales (i.e. 20 and 1000 s, or 12 and 540 m), fluorescence also exhibits a very specific spectral behaviour, independent of the physical forcings, with $\beta \approx 0.66$. This result roughly fits with theoretical and experimental results (Powell *et al.*, 1975;

Denman and Platt, 1976; Denman *et al.*, 1977; Bennett and Denman, 1985; Steele and Henderson, 1992; Powell and Okubo, 1994) predicting that the phytoplankton biomass spectrum will be flatter than the spectrum of a scalar contaminant of the flow field and indicating that in this region different processes contribute to the variance of phytoplankton biomass, i.e. that temporal variability in the biological parameters such as cell growth and community structure has an important role in shaping the phytoplankton biomass distribution.

On the other hand, for scales larger than 1000 s (or 540 m), the spectral exponents β are obviously larger than the theoretical β ≈ 5/3 (modified *t*-test, $P > 0.05$; Scherrer, 1984) and the spectral exponent of salinity appears significantly larger than the exponents of temperature and the fluorescence, which cannot be distinguished (Tukey multiple comparison test, $P < 0.05$; Zar, 1996). This scaling behaviour, obviously independent of turbulent processes, may then qualitatively (we try a quantification latter) be related to the very specific structuration of the hydrological pattern of the Eastern English Channel. Indeed, the megatidal regime and the fluvial supplies distributed from the Bay of Seine to Cape Griz-Nez along the French coast generate a heterogeneous coastal water mass which drifts nearshore, separated from the open sea by a frontal area (Brylinski and Lagadeuc, 1990; Lagadeuc *et al.*, 1997)—known as the 'coastal flow' (Brylinski and Lagadeuc, 1990; Brylinski *et al.*, 1991)—and characterized by its freshness, turbidity (Dupont *et al.*, 1991) and phytoplankton richness (Quisthoudt, 1987; Brylinski *et al.*, 1991). The very specific scaling behaviour previously described can then be associated both with the coastal heterogeneity related to the progressive integration of freshwater inputs to marine waters (Brylinski *et al.*, 1991; Lagadeuc *et al.*, 1997) and with the influence of a frontal area, as suggested by the closeness of the scaling exponent β with the theoretical β ≈ 2 expected in the case of frontal mixing (Kraichnan, 1967; Bennett and Denman, 1985).

Multifractality of oceanic turbulent fields. The computations of the temperature, salinity and *in vivo* fluorescence structure functions (i.e. $<(\Delta T_\tau)^q>$, $<(\Delta S_\tau)^q>$ and $<(\Delta F_\tau)^q>$, respectively) confirm the scaling regimes previously shown by spectral analysis for different orders of moments q (Figure 15). The slopes, fitted to the data by least squares over the range of scale values for which the data are scaling (i.e. the curves are linear), provide estimates of the exponents $\zeta(q)$.

The scaling of the first moment $\zeta(1)$ $[\zeta(1) = H]$ for temperature, salinity (over scales smaller than 1000 s, or 540 m) and fluorescence (over scales smaller than 20 s, or 12 m) are not significantly different (Analysis of Covariance, $P < 0.05$; Zar, 1996), with $\zeta(1) = 0.40 \pm 0.01$, $\zeta(1) = 0.38 \pm 0.01$ and $\zeta(1) = 0.43 \pm 0.01$, respectively. Here, as below, the error bars come from the different portions of the dataset analysed separately: for example, with the scaling of temperature and salinity up to 1000 s and a database of 167 040 points, we can estimate the exponents for 167 non-overlapping intervals. For scales larger than 1000 s, the scaling exponents H (see Table I) appear significantly different for the temperature, salinity and fluorescence fields (Analysis of Covariance, $P > 0.05$; Zar, 1996), the scaling exponents being significantly larger for salinity than those related to temperature and fluorescence, which remain indistinguishable (Tukey multiple
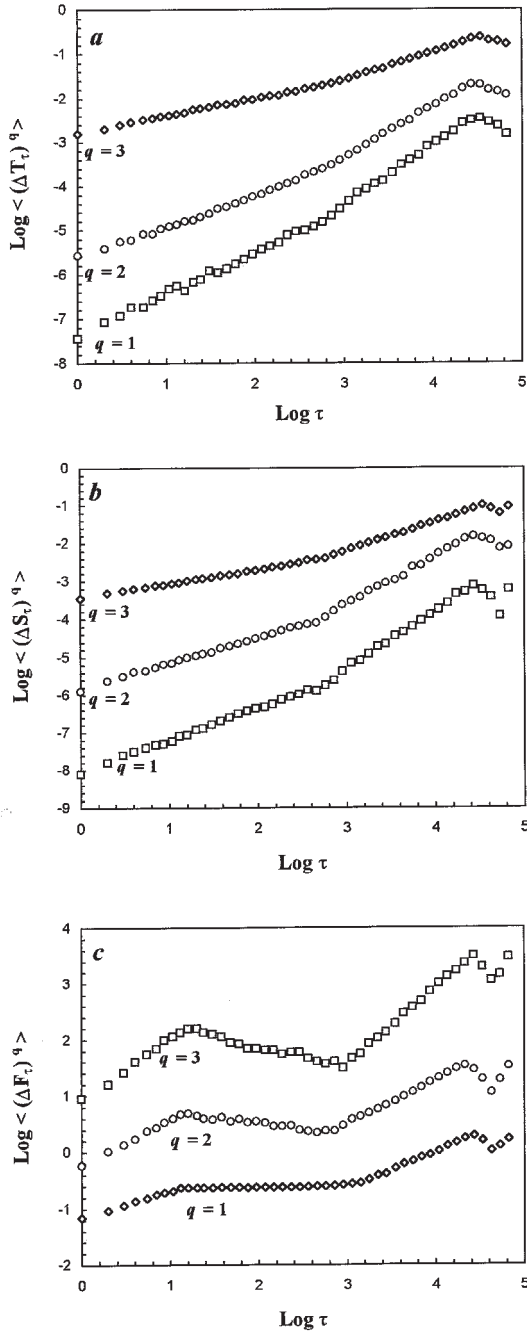
Fig. 15. The structure functions $<(\Delta T_\tau)^q>$, $<(\Delta S_\tau)^q>$ and $<(\Delta F_\tau)^q>$ versus τ in log–log plots for $q = 1$, 2 and 3 for temperature (**a**), salinity (**b**) and *in vivo* fluorescence (**c**). Two and three linear trends are clearly visible on the one hand for temperature and salinity, and on the other hand for *in vivo* fluorescence (see Table I for slope estimates).

Table I. Empirical estimates of the spectral exponent β, and the first and second moment scaling exponent ζ(1) = H and ζ(2) for temperature, salinity and *in vivo* fluorescence for the different scaling regimes encountered

	$t < 20$ s			$20 < t < 1000$ s			$t > 1000$ s		
	H	$\zeta(2)$	β	H	$\zeta(2)$	β	H	$\zeta(2)$	β
Temperature	0.40	0.71	1.72	0.40	0.71	1.72	0.64	0.97	1.98
Salinity	0.38	0.67	1.67	0.38	0.67	1.67	0.80	1.22	2.25
Fluorescence	0.43	0.75	1.77	0.00	–0.35	0.66	0.66	0.97	1.96

Table II. Empirical estimates of the universal multifractal parameters C_1 and α for temperature, salinity and *in vivo* fluorescence for the different scaling regimes encountered

	$t < 20$ s		$20 < t < 1000$ s		$t > 1000$ s	
	C_1	α	C_1	α	C_1	α
Temperature	0.05	1.90	0.05	1.90	0.24	1.35
Salinity	0.05	1.90	0.05	1.90	0.27	1.50
Fluorescence	0.06	1.80	0.20	1.60	0.24	1.37

comparison test, $P < 0.05$; Zar, 1996). Over intermediate scales (i.e. from 20 to 1000 s), *in vivo* fluorescence structure functions $<(\Delta F_\tau)^q>$ for the first order of moment show no slope, i.e. $\zeta(1) = H \approx 0$, indicating a conservative behaviour (i.e. fluctuations of fluorescence are scale independent). In the same way, the scaling of the second-order moments confirms the estimates of β from the power spectra $[\beta = 1 + \zeta(2)]$ for each scaling regime (cf. Table II).

More generally, the non-linearity of the empirical curve $\zeta(q)$ in Figure 16 shows that these different fields can be considered as multifractals; the curves corresponding to temperature and *in vivo* fluorescence (i.e. phytoplankton biomass) are very close to each other for scales smaller than 1000 s and 20 s, respectively (Figure 16a and b), and for scales larger than 1000 s (Figure 16d and e). Within experimental error, they cannot be qualitatively (we try a quantification later) showed as being different. On the contrary, the empirical curves $\zeta(q)$ for salinity (Figure 16c and f) are slightly different, showing more convex behaviours, especially on large scales (Figure 16f), whereas *in vivo* fluorescence $\zeta(q)$ exhibits a very specific behaviour (Figure 17) over scales between 20 and 1000 s. It can be noticed that the empirical moment scaling exponent $K(q)$, obtained by the estimates of the slopes of the linear trend of $<(\Phi_l)^q>$ versus l in a log–log plot (Figure 18a) from equation (15), clearly exhibits multifractal properties previously described (Figure 18b; cf. Figure 8) and confirms the link existing between the exponents $K(q)$ and $\zeta(q)$ given by equations (17) and (22) (Figure 18b).

Universality of turbulent oceanic fields. We realize a quantitative description of scale invariant fields computing estimations of universal parameters and using the DTM analysis technique (Lavallée, 1991; Lavallée *et al.*, 1992), basically applied to a great variety of geophysical data (Schmitt *et al.*, 1992a,b, 1993; Teissier *et al.*,
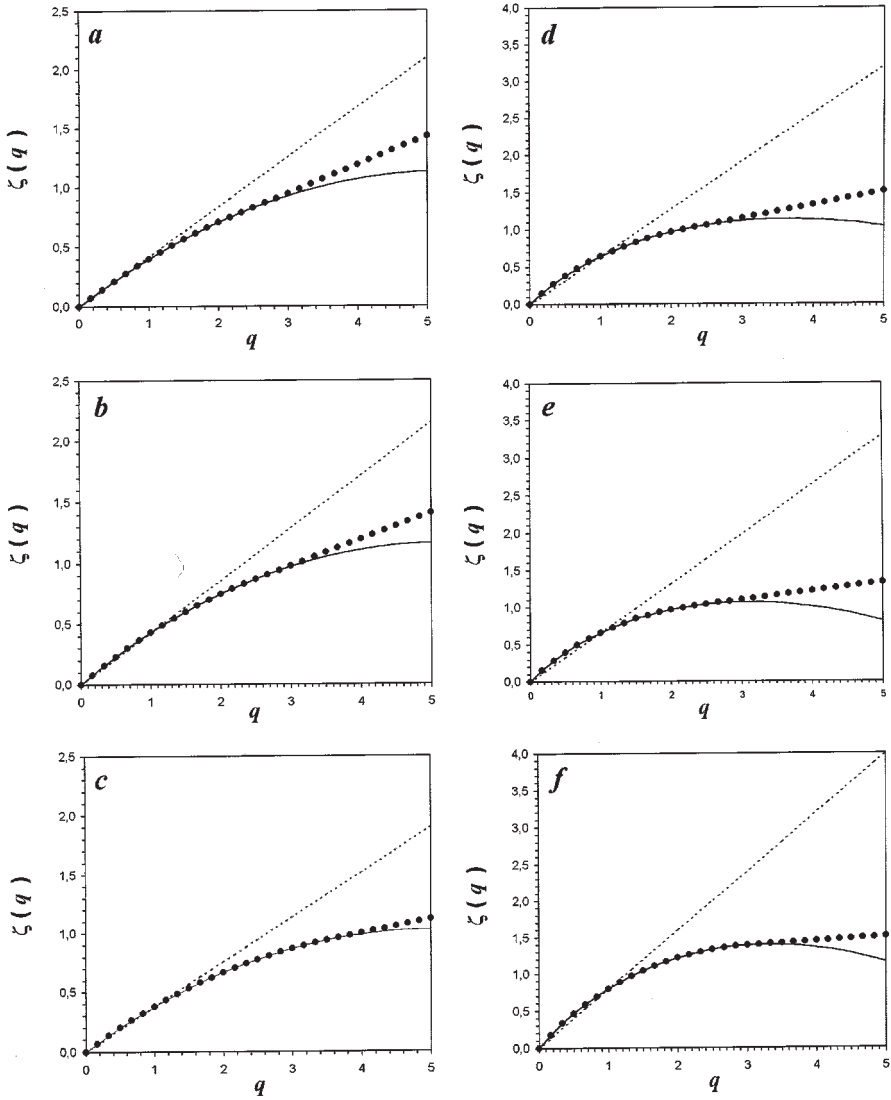
Fig. 16. The scaling exponent structure function $\zeta(q)$ empirical curves (dots), compared to the monofractal curves $\zeta(q) = qH$ (dashed line), and to the universal multifractal curves (continuous curve) obtained with C_1 and α (cf. Table II) in equation (22) for temperature, salinity and *in vivo* fluorescence over small scales (i.e. scales smaller than 1000 s for temperature and salinity, and smaller than 20 s for *in vivo* fluorescence) and large scales (i.e. scales >1000 s). The empirical curves are non-linear, indicating multifractality.

1993a,b; Chigirinskaya *et al.*, 1994, 1997; Lazarev *et al.*, 1994; Falco *et al.*, 1996), based on multiscaling properties of the intermittent fluxes Φ_λ (i.e. obtained by fractional differentiation of order H) of temperature, salinity and fluorescence fields as defined in equation (19). The scaling of the intermittent fluxes $<(\phi_{\lambda,\Lambda}^\eta)^q>$ (Figure 19) is shown for $q = 2$ and different values of η. The slopes of $<(\phi_{\lambda,\Lambda}^\eta)^q>$
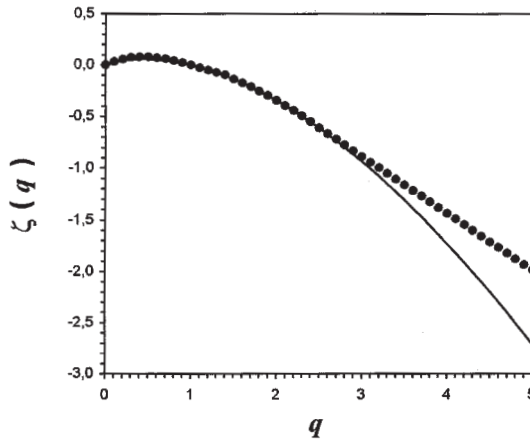
**Fig. 17.** The scaling exponent structure function $\zeta(q)$ empirical curves (dots), compared to the universal multifractal curve obtained with C_1 and α (cf. Table II) in equation (22) for *in vivo* fluorescence for scales bounded between 20 and 1000 s, where biological activity has an important role in shaping the phytoplankton biomass distribution.

versus λ in a log–log plot, fitted by least squares, are the estimates of $K(q, \eta)$. The linear trends of the curves $K(q, \eta)$ versus η, plotted in a log–log graph, show that equation (25) is well respected for a wide range of η values (Figure 20). Their slopes and the intercepts give, respectively, the estimates of α and C_1, wholly presented in Table II, and suggest an increasing heterogeneity and a decreasing multifractality from small to large scales for both physical and biological parameters, globally leading to view the distributions of these parameters as more patchy distributed on larger scales.

To test the validity of the estimates of α and C_1 of the intermittent fields, we fit the empirical scaling exponent $\zeta(q)$ with the theoretical universal multifractal expression given by α and C_1 (Table II) in equation (22). The universal multifractal and empirical fits are excellent until critical moment of order q_c (Table III), after which the empirical curves are linear (Figures 16 and 17). This linear behaviour of the empirical scaling exponent structure function $\zeta(q)$ is known for sufficiently high-order moments (Schertzer and Lovejoy, 1989) and is due to sampling limitations (i.e. second-order multifractal phase transition; Schertzer and Lovejoy, 1992) or is associated with a divergence of statistical moments (i.e. first-order multifractal phase transition; Schertzer and Lovejoy, 1992) if substantiated by large enough sample size. In both cases, for $q \geq q_c$, the empirical $\zeta(q)$ follows:

$$\zeta(q) = 1 - \gamma_{max}q \qquad (26)$$

where γ_{max} is the maximum singularity associated to q_c. In the case of a first-order phase transition, q_c corresponds specifically to maximum singularity measured, which is associated with the occurrence of very rare and violent singularities, whereas in the case of a second-order multifractal phase transition, q_c corresponds
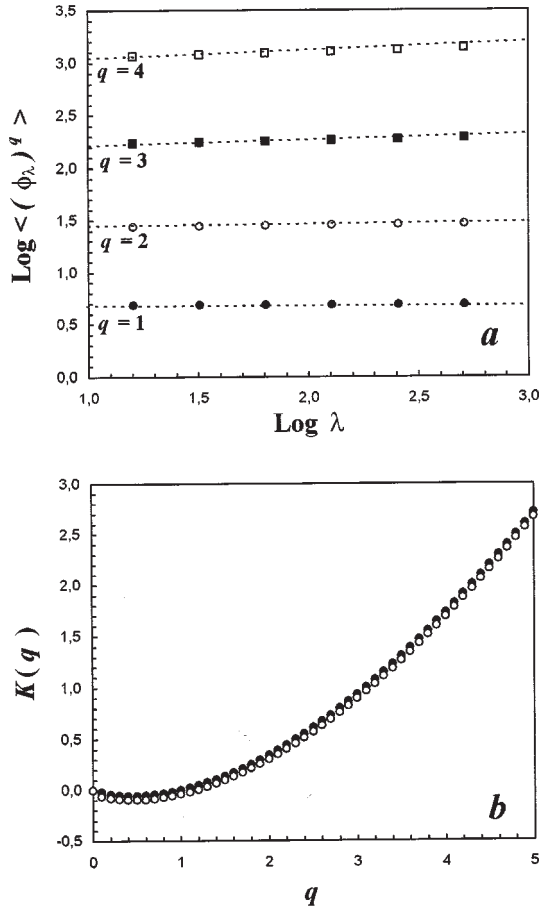
Fig. 18. The curves $<(\varphi_\lambda)^q>$ versus λ in a log–log plot for *in vivo* fluorescence for scales ranging from 20 to 1000 s (**a**). The slopes of straight lines indicating the best regression over the range of scales provide estimates of the empirical scaling exponent $K(q)$ [(**b**), dark circles; cf. equation (15)] which is compared to the $K(q)$ estimated following $K(q) = qH - \zeta(q)$ [open circles; cf. equation (22)].

to the maximum singularity effectively measurable from a finite sampling [see Schmitt *et al.* (1994) for further developments].

In order to differentiate between first and second multifractal phase transitions, we then compute the theoretical value of the critical moment q_s expected in the case of sampling limitations given by (Schertzer and Lovejoy, 1992):

$$q_s = \left(\frac{1}{C_1} \right)^{1/\alpha} \tag{27}$$

and compare it with the q_c estimated from the empirical $\zeta(q)$ (see Figures 16 and 17). With the values of α and C_1 estimated above (Table II), we obtain q_s values

903
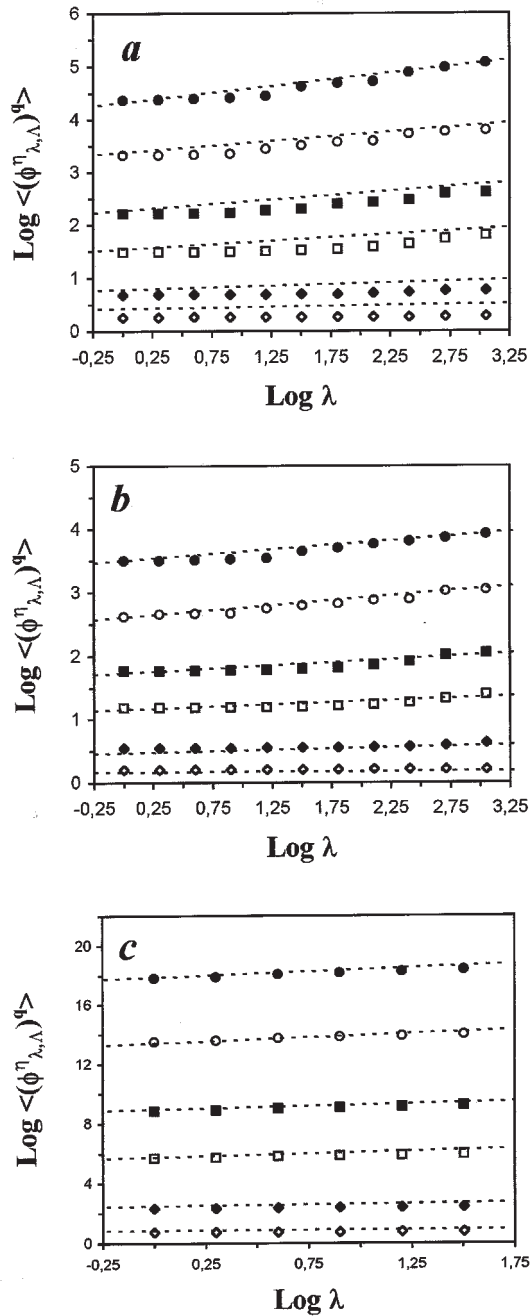
Fig. 19. The curves $<(\phi^{\eta}_{\lambda,\Lambda})^q>$ versus λ for temperature (**a**), salinity (**b**) and *in vivo* fluorescence (**c**) over small scales (i.e. scales smaller than 1000 s for temperature and salinity, and smaller than 20 s for *in vivo* fluorescence) shown in a log–log plot for $q = 2.5$ and for different values of η ($\eta = 0.2, 0.5, 1, 1.4, 2$ and 2.5 from bottom to top). The slope of the linear trends provides estimates of the double trace moment scaling exponent $K(q, \eta)$ [cf. equation (23)].

904
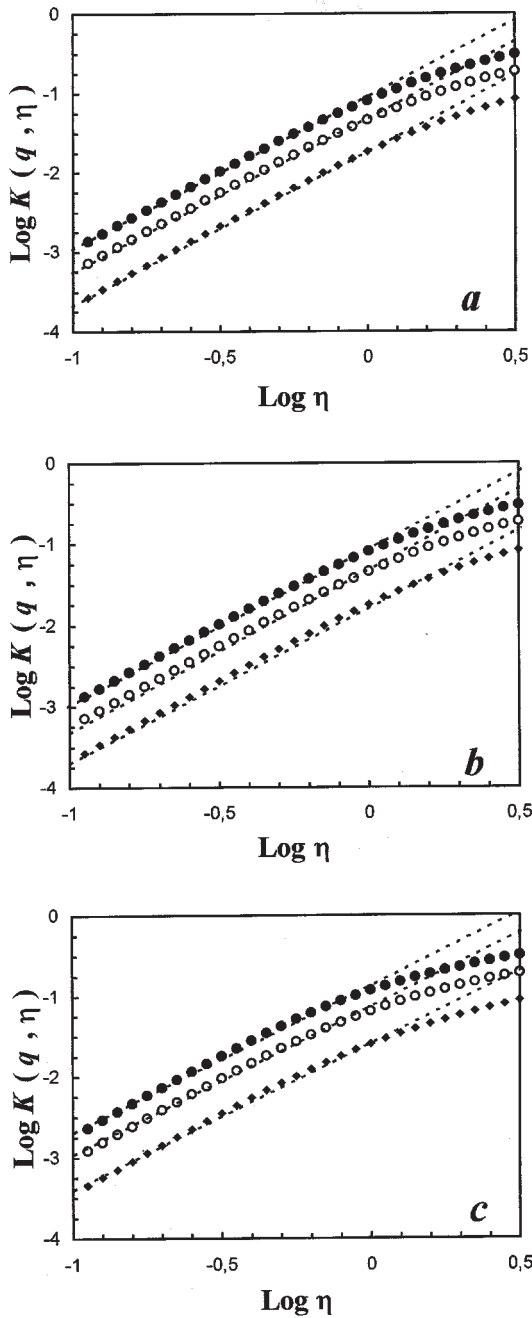
Fig. 20. The curves $K(q, \eta)$ versus η in a log–log plot for $q = 2.5$ and 3 (from bottom to top) for temperature (**a**), salinity (**b**) and *in vivo* fluorescence (**c**), where $K(q, \eta) = \eta^\alpha K(q)$. The slope of the straight lines then gives the estimates of α and C_1 is estimated by the intercept.

very close to the values estimated from the empirical curves $\zeta(q)$ for intermediate and large-scale fluorescence, but also for temperature and salinity for scales larger than 1000 s ($q_c \approx q_s$). Those critical moments are therefore only linked to sampling limitations (i.e. second-order multifractal phase transition), because we had to average the original time series up to the scale of 20 and 1000 s, in order to be in the appropriate ranges of scales. On the contrary, on smaller scales, the situation is obviously different with $q_c < q_s$, clearly indicating that the critical moments q_c are independent of sampling and characterizing the occurrence of very rare and violent singularities in our dataset (i.e. first-order multifractal phase transition).

Those results, showing the extreme similarity of temperature, salinity and fluorescence field on small scales (see Tables I, II and III), can be regarded as a quantitative verification of the hypothesis of small-scale fluorescence as being a purely passive scalar and generalization of previous works which tested the passivity assumption using only power spectra (i.e. a second-order moment). Furthermore, the very specific non-linear behaviour of the structure functions scaling exponent $\zeta(q)$ for *in vivo* fluorescence over scales ranging from 20 to 1000 s as the differences perceived in temperature, salinity and fluorescence distributions for scales larger than 1000 s indicate that variability can also be wholly described in a universal multifractal framework even over scales dominated by non-turbulent processes.

Discussion

Scales of patchiness for intermittent fields in turbulent coastal waters

Small scales. The present case study has shown that on small scales (i.e. < 20 s, or 12 m, for *in vivo* fluorescence and < 1000 s, or 540 m, for temperature and salinity), *in vivo* fluorescence, temperature and salinity spectral behaviours are statistically indistinguishable and closely follow the –5/3 power law derived by Kolmogorov (1941) for the inertial subrange of turbulent velocity fields. This is the region of the turbulence spectrum where energy transferred from larger eddies (i.e. large-scale eddies induced by external forcings such as wind and tidal patterns) to the smallest eddies which dissipate their energy into heat (i.e. viscous dissipation cannot be neglected and smooth out turbulent fluctuations). That implies that the distribution of phytoplankton was governed primarily by the turbulent environment, and not by the net growth rate (which includes division and predation) of cells themselves. One may note here that in the case of interacting species (i.e. intra- and interspecific interactions), the power spectrum of phytoplankton biomass fluctuations should have exhibited a steeper slope, even for the inertial subrange (i.e. $\beta = 3$; Powell and Okubo, 1994).

Subsequent multifractal analysis confirms and generalizes these observations. Indeed, the relative commonality of the estimates of the three basic universal multifractal parameters, H, C_1 and α—but also the critical moments q_c—of temperature, salinity and phytoplankton biomass, then reflects profound couplings between space–time structure of phytoplankton populations and the structure of their physical environment (see Tables II and III), as previously

Table III. Theoretical and empirical estimates of the critical moment q_s for temperature, salinity and *in vivo* fluorescence for the different scaling regimes encountered

	$t < 20$ s		$20 < t < 1000$ s		$t > 1000$ s	
	q_s (theoretical)	q_s (empirical)	q_s (theoretical)	q_s (empirical)	q_s (theoretical)	q_s (empirical)
Temperature	4.84	2.50	4.84	2.50	2.88	2.80
Salinity	4.84	3.20	4.84	3.20	2.39	2.50
Fluorescence	4.77	2.70	2.73	2.80	2.83	2.75

suggested by simple representations of the extreme intricacy between the space–time scales of physical and biological marine processes (Stommel, 1963; Haury *et al.*, 1978; Steele, 1978; Marquet *et al.*, 1993). Furthermore, the universal multifractal parameters H, C_1 and α obtained from the present study (cf. Table II) appear very similar to those obtained from previous studies conducted in different water masses and tidal conditions (Table IV). This suggests that the small-scale variability of phytoplankton biomass, wholly characterized in terms of multifractality, cannot be regarded as density dependent, as previously found by Prairie and Duarte (1996) in a various set of marine and freshwater phytoplankton distribution. One may also note that the difference between the estimates of H, C_1 and α observed during spring and neap tides (cf. Table IV) did not suggest any tidal dependence of the distribution of both physical and biological parameters. However, in a recent monofractal study of vertical phytoplankton variability also conducted in the coastal waters of the Eastern English Channel, Seuront and Lagadeuc (1998) showed both a density dependence and a tidal dependence of phytoplankton biomass distribution associated with the inshore–offshore hydrological gradient and the flood/ebb alternance, respectively. This study, involving narrower ranges of spatio-temporal scales, then cannot be directly compared with the present results. Further investigations are therefore still needed to identify the relative effects of different advection processes and hydrodynamics on the structuration of phytoplankton biomass variability, for instance by considering shorter datasets differentially distributed over a whole tidal cycle, but it was not the aim of this paper.

The examination of the critical moments q_c (Table III) led to further conclusions. Indeed, our results showed that during a period of spring tide $q_c < q_s$ [where q_c and q_s are the empirical moments after which the scaling exponent $\zeta(q)$ is linear, and the theoretical critical moment characterizing sampling limitations, respectively], while similar studies conducted during a period of neap tide (Seuront *et al.*, 1996a) rather suggest $q_c \approx q_s$ [$q_s \approx 6.0$, with $C_1 = 0.04$ and $\alpha = 1.80$ in equation (27) for phytoplankton biomass]. This could, therefore, suggest a differential intermittent behaviour of physical (i.e. temperature and salinity) and biological (i.e. phytoplankton biomass) variability in spring and neap tides. Spring tide physical and biological variability are characterized by more violent events than during neap tide. Such a difference in the occurrence of extreme events between different hydrodynamic conditions may be of prime interest in future studies in planktonology following the recent emphasis on understanding

Table IV. Values of the universal multifractal parameters H, C_1 and α obtained by Seuront *et al.* (1996b) in the Eastern English Channel at the end of March 1995 during a period of spring tide (a), by Seuront (1997) and Seuront *et al.* (1996a) in the Southern Bight of the North Sea in June 1991 during periods of neap tide (b and c, respectively), and compared to the values obtained in the present study (d). The values of the slopes of the Fourier power spectra β are also indicated

(a)

	$t < 13$ s			
	β	H	C_1	α
Temperature	1.65	0.34	0.035	1.70
Salinity	–	–	–	–
Fluorescence	1.66	0.36	0.035	1.80

(b)

	$t < 100$ s				100 s $< t < 6$ h			
	β	H	C_1	α	β	H	C_1	α
Temperature	1.75	0.41	0.05	1.75	1.75	0.41	0.05	1.75
Salinity	–	–	–	–	–	–	–	–
Fluorescence	1.78	0.43	0.045	1.85	–	–	–	–

(c)

	$t < 100$ s				100 s $< t < 12$ h			
	β	H	C_1	α	β	H	C_1	α
Temperature	1.74	0.42	0.04	1.70	1.74	0.04	0.05	1.70
Salinity	–	–	–	–	–	–	–	–
Fluorescence	1.75	0.41	0.04	1.80	1.22	0.12	0.02	0.80

(d)

	$t < 20$ s				$20 < t < 1000$ s				1000 s $< t < 48$ h			
	β	H	C_1	α	β	H	C_1	α	β	H	C_1	α
Temperature	1.72	0.40	0.05	1.90	1.72	0.40	0.05	1.90	1.98	0.64	0.24	1.35
Salinity	1.67	0.38	0.05	1.90	1.67	0.38	0.05	1.90	2.25	0.80	0.27	1.50
Fluorescence	1.77	0.43	0.06	1.80	1.66	0.00	0.20	1.60	1.96	0.66	0.24	1.37

detailed mechanisms that determine each individual feature (Yamazaki, 1993; Paffenhöfer, 1994). Moreover, one may note here that our multifractal approach provides a very precise statistical description of the studied processes (i.e. estimates of all moments, even non-integers, up to moment of order 5), while the characterization of other non-Gaussian empirical data or processes is basically limited to their three first moments (average, variance and skewness).

This demonstrated small-scale structured (i.e. non-random) distribution of phytoplankton biomass should therefore constitute an important subset in the growing field of determining the influence of turbulence on plankton ecosystems

(e.g. Costello *et al.*, 1990; Marrasé *et al.*, 1990; Granata and Dickey, 1991; Yamazaki and Kamykowski, 1991; Madden and Day, 1992; Kiørboe, 1993). Indeed, it is noteworthy that the present understanding of turbulence incorporated into most aspects of marine and freshwater biology is that turbulence has an essentially random effect on transport. This view is predicated on the assumption that transport in a turbulent flow is similar to molecular transport and diffusion, and is consequently reflected in plankton transport models (Okubo, 1986; Rothschild and Osborn, 1988; Yamazaki, 1993), as well as other areas in which turbulence is important (McCave, 1984; Davis *et al.*, 1991; Yamazaki and Haury, 1993). Moreover, heterogeneous particle distributions, such as the very specific phytoplankton distribution analysed here in the universal multifractal framework, may also have salient consequences, as demonstrated by Currie (1984) on the basis of Taylor approximations of the Michaelis–Menten function, on non-linear concentration-dependent processes such as phytoplankton coagulation (Riebesell, 1991a,b; Kiørboe *et al.*, 1994; Kiørboe, 1997), the encounter of a mate during sexual reproduction (Waite and Harrison, 1992), the encounter rates between a zooplanktonic predator and its prey (Rothschild and Osborn, 1988; Sundby and Fossum, 1990; MacKenzie *et al.*, 1994; Raby *et al.*, 1994; Kiørboe and MacKenzie, 1995; MacKenzie and Kiørboe, 1995), and then may provide new perspectives in the research on primary and secondary production.

Another salient consequence suggested by our results is that turbulent processes cannot be regarded as log–normally distributed, as propounded by many workers (Gregg *et al.*, 1973; Belyaev *et al.*, 1975; Osborn, 1978; Elliott and Oakey, 1979; Gregg, 1980; Wasburn and Gibson, 1984; Oakey, 1985; Osborn and Lueck, 1985a,b; Baker and Gibson, 1987; Gibson, 1991). Log–normal distribution being a particular case of multifractal distribution [i.e. $\alpha = 2$ in equations (17) and (22)], our universal multifractal characterization of small-scale temperature and salinity variability therefore indicates another level of structuration of turbulent fluid motions. Universal multifractal and log–normal distributions can be regarded as belonging to a particular family of skewed distributions reflecting a heterogeneous distribution with a few dense patches and a wide range of low-density patches. This means that occasionally we should expect stronger bursts, more often than in the Gaussian case, characterizing intermittent processes. The phenomenon of intermittency, which is discussed in more detail elsewhere (Jiménez, 1997; Jou, 1997), has recently been shown to be associated with the presence of strong coherent vortices, with diameter of the order of 10 times the Kolmogorov scale (i.e. the Kolmogorov length scale), but with much longer lengths and probably long lifetimes (Jiménez *et al.*, 1993; Jiménez and Wray, 1994).

Coarse scales. On coarser scales (i.e. 20–1000 s, or 12–540 m), the power spectrum of phytoplankton density fluctuations is flatter (i.e. 'whiter') than the –5/3 energy spectrum, i.e. the intensity of patchiness is less than that of environmental turbulence fluctuations. Denman and Platt (1976) and Denman *et al.* (1977) first described these relationships for the inertial subrange. They defined three distinct regions in the phytoplankton biomass power spectrum. If τ (s) represents the time

taken for a turbulent eddy to transfer its energy to an eddy half its size, and μ (s^{-1}) is the doubling rate of the phytoplankton, then for μ^{-1} >> τ, the growth rate of the phytoplankton is insufficient to produce a spatio-temporal distribution that is different from that of purely passive quantities such as temperature or salinity. The phytoplankton behave as passive tracers; thus, the slope of the power spectrum of phytoplankton density fluctuations is similar to that for environmental fluctuations, both in the inertial subrange (β ≈ 5/3) and in two-dimensional turbulence (β ≈ 3; Gower *et al.*, 1980; Deschamps *et al.*, 1981; Abraham, 1998). However, for μ^{-1} << τ, the phytoplankton are doubling sufficiently quickly for their spatio-temporal distribution to be no longer nullified by turbulence. The spatio-temporal structure of the community cannot be destroyed by the diffusive action of the eddies, and in this case theoretical curves indicate a flattening of the phytoplankton biomass spectrum, i.e. β ≈ 1, both in the inertial subrange (Denman and Platt, 1976; Denman *et al.*, 1977) and in two-dimensional turbulence (Bennett and Denman, 1985; Powell and Okubo, 1994). For μ^{-1} ≈ τ, a transitional regime where neither process dominates occurs, and the spatial patterns formed may be the result of a complex interaction between τ and μ. This transition zone corresponds to the minimum patch which can maintain itself in the face of diffusion, known as the KISS length (Okubo, 1978, 1980). The relationship between τ and μ has been further quantified by Denman *et al.* (1977), who proposed a critical patch size for phytoplankton in the open ocean of 5–10 km, while other theoretical studies have derived a characteristic patch size of 1–2 km for phytoplankton populations in bloom conditions (e.g. Okubo, 1980).

Yet, the interpretation of the proximal cause of small-scale plankton patchiness has then been in terms of population growth rather than aggregation of organisms which grew elsewhere. However, one may note here that the characteristic time and space scales associated with the flattening of our phytoplankton biomass spectrum (i.e. 1000 s, or 540 m) occurs for scales significantly smaller than the generation time of phytoplankton populations (i.e. ≈ 1 day) and the critical patch size found in the literature. In that way, comparisons of our universal multifractal distribution of phytoplankton biomass ζ(q) (cf. Figure 17) to the structure function scaling exponent ζ$_F$(q) = −K(q/2) of a biologically active scalar derived by Seuront *et al.* (1996b) from the previous theoretical results of Denman and Platt (1976) and Denman *et al.* (1977) then lead to further conclusions. Phytoplankton distributions observed in the Eastern English Channel and in the Southern Bight of the North Sea, respectively, over time scales ranging from 20 to 1000 s (i.e. 12–540 m) and for time scales >100 s (i.e. 30 m) (Table IV; Seuront *et al.*, 1996a), are obviously different from the theoretical curve ζ$_F$(q) (Figure 21). This suggests that aggregation processes occurring over these ranges of scales cannot be strictly associated with phytoplankton growth rates. Indeed, field studies frequently suggest that plankton aggregations can also be associated with hydrodynamic discontinuities such as fronts and eddies (Alldredge and Hammer, 1980; Mackas *et al.*, 1980; Herman *et al.*, 1981; Owen, 1981), while some theoretical studies proposed patch-generating mechanisms associated with Langmuir cells (Stommel, 1949; Stavn, 1971), internal waves (Kamykowski, 1974), tidal current shear (Riley, 1976), wind-driven currents (Verhagen, 1994) and grazing activity

(Evans, 1978). In the present case, plankton patches are obviously too small in spatial dimension and too transitory in duration to be the results of reproductive population increase. This suggests another level of complexity in the patch-generating mechanisms, such as complex interactions between the turbulence level of fluid motions (e.g. different tidal and wind conditions), the phytoplankton biomass concentration and the specific composition of phytoplankton assemblages, highly variable all along the year in the Eastern English Channel and in the Southern Bight of the North Sea (Martin-Jezequel, 1983; Gentilhomme and Lizon, 1998). This seems indeed to be the case following the differences observed in the universal multifractal parameters between exeriments conducted in the Eastern English Channel during a period of spring tide (i.e. $H = 0.00$, $C_1 = 0.20$ and $\alpha = 1.60$; present study), and the Southern Bight of the North Sea ($H = 0.12$, $C_1 = 0.02$ and $\alpha = 0.80$; Seuront et al., 1996a). Phytoplankton biomass then appears to be more conservative (i.e. low H value, the mean of the fluctuations is then less scale dependent, indicating a reduced flux from large to small scales), more heterogeneously distributed (i.e. high C_1 value corresponding to sparse patches) and structured (i.e. high α value indicating a higher multifractality, that is to say the occurrence of numerous intermittency levels between maximum and minimum concentrations) in the Eastern English Channel than in the North Sea. Whatever that may be, further investigations are still needed to estimate the relative importance of hydrodynamic, hydrological, seasonal processes and their related populational, biological and physiological effects on the precise structure of phytoplankton fields.

At larger scales (i.e. >1000 s, or 540 m), the situation is quite different, phytoplankton biomass variability appearing essentially similar to temperature variability, suggesting a decoupling between phytoplankton and salinity dynamics.
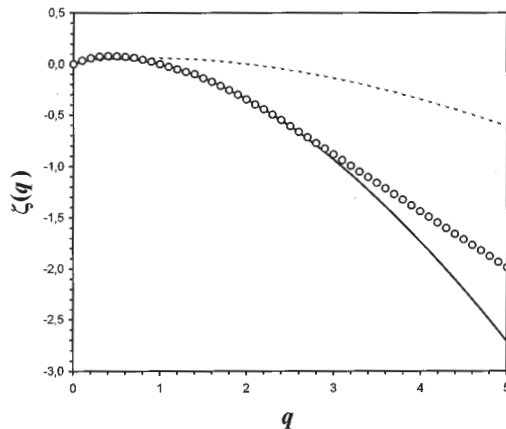
Fig. 21. The empirical structure function scaling exponent $\zeta(q)$ estimated for *in vivo* fluorescence for scales ranging from 20 to 1000 s (continuous curve) compared to the universal multifractal functions obtain with C_1 and α in equation (22) (open circles) and to the theoretical formulation for $\zeta(q)$ proposed by Seuront et al. (1996b) as an extension of previous spectral and dimensional theoretical works by Denman and Platt (1976) and Denman et al. (1977) (dashed curve).

Then, over this range of scales, river inflow cannot be directly regarded as a source of phytoplankton biomass variability, which seems to be rather controlled by mixing processes associated with the frontal area separating inshore and offshore waters, as suggested by the very specific spectral behaviour (i.e. $\beta \approx 2$; Kraichnan, 1967; Bennett and Denman, 1985) and the extreme similarity existing between the universal multifractal parameterization of temperature and *in vivo* fluorescence (cf. Table II). However, both the coastal heterogeneity in salinity related to the progressive integration of freshwater inputs to marine waters (Brylinski *et al.*, 1991; Lagadeuc *et al.*, 1997) and the haline stratification existing at the mouth of estuaries which maintains nutrient-rich waters favouring the initiation of phytoplankton blooms (Pingree *et al.*, 1986) can also be regarded as potential sources of heterogeneity in the coastal distribution of phytoplankton biomass in this area. In that way, one may also note that the occurrence of a joint transition zone for these three parameters demonstrates that the scales of the physics and biology were nearly coincident, even when the interactions are not necessarily closely coupled. This could suggest a differential physical control of phytoplankton biomass distribution, the precise nature of these interactions remaining unresolved. The values of the universal multifractal parameters, H, C_1 and α (see Table II), nevertheless indicate a more patchy distribution of temperature, salinity and phytoplankton biomass in comparison with the scales dominated by tri-dimensional turbulent processes (i.e. the inertial subrange) where heterogeneity was very low (i.e. C_1 values) and multifractality approached its upper limit (i.e. $\alpha \approx 2$).

Multifractal analysis: a new way of looking across scales for intermittent processes

The different transition zones separating the previously described partial scaling behaviours indicate characteristic scales where the environmental properties or constraints acting upon organisms, or more generally the structure of the variability of a given field, are changing rapidly (Frontier, 1987; Seuront and Lagadeuc, 1997). The concepts of 'scale' and 'pattern' being ineluctably intertwined (Hutchinson, 1953), the identification of scales, which is at the core of our thought process, then appears to be essential to the identification and characterization of patterns (Legendre and Fortin, 1989; Wiens, 1989; Jarvis, 1995). The problem of scale has fundamental applied importance in ecosystem modelling. Until now, the study of population variability has required the selection of an appropriate region of the space–time domain (Steele, 1988). For instance, the general circulation models that provide the basis for climate prediction (Hansen *et al.*, 1988), as well as the regional circulation models (Nihoul and Djenidi, 1991; Salomon and Breton, 1993), operate on spatial and temporal scales many orders of magnitude greater than the scales at which most ecological processes, such as physiological and behavioural responses of phytoplankton and zooplankton, occur. Moreover, the development of new observation techniques such as remote sensing, while providing very exciting images of surface patterns of both chlorophyll and temperature over a wide range of scales (Abbott and Zion, 1985, 1987;

Denman and Abbott, 1988), must also lump functional ecological classes, sometimes into very crude assemblages, suppressing considerable detail, whereas ecological studies require that we sample spatially and temporally as fully as possible (see, for example, Platt *et al.*, 1989). By interfacing individual-based models with fluid dynamics models, therefore, one seeks to interrelate phenomena acting on different scales (Billen and Lancelot, 1988; Sharples and Tett, 1994; Zakardjian and Prieur, 1994), but it is still necessary to have available a suite of models of different levels of complexity and to understand the consequences of suppressing or incorporating details. Actual key challenges in the study of ecological systems therefore involve ways to deal with the collective dynamics of heterogeneously distributed ensembles of individuals, and to understand how to relate phenomena across scales, i.e. to scale from small to large spatio-temporal scales (Auger and Poggiale, 1996; Levin *et al.*, 1997; Poggiale, 1998a,b).

However, the development of theoretical models which incorporate multiple scales and which will guide the collection and the interpretation of data is still lacking because of the insufficiency of techniques to look across scales (Steele, 1991). This is the major contribution of fractal geometry (Mandelbrot, 1977, 1983; Frontier, 1987; Milne, 1988; Sugihara and May, 1990a), which is recognized to be capable of describing how patterns change across scales. Then, basically assuming that there is no single scale at which ecosystems should be described, there is no single scale at which models should be constructed (Levin, 1992). Furthermore, Bellehumeur *et al.* (1997) showed that an ecological phenomenon spread out in space and time does not have discrete spatial scales, but a continuum of spatio-temporal structures whose perception depends on the size of the sampling units, an assumption which greatly agrees with our multiscale approach. Consequently, ecological processes seem to be better described by a continuum of scales rather than a hierarchy of overlapped scales (Allen and Starr, 1982; O'Neill, 1989; Allen and Hoekstra, 1991; O'Neill *et al.*, 1991). In such a background, universal multifractal formalism, leading to a very precise characterization of variability by the way of continuous multiplicative processes (with the help of the three basic empirical parameters), appears to be an efficient descriptive tool which should also allow the modelling of the multiscale detailed variability of intermittently fluctuating biological fields as the global properties of their surrounding physical environment. Indeed, multifractal approaches are much better than the usual approaches which give a description at a very limited range of scales. One may note that models or direct numerical simulations possess no way to change the scale upward (upscaling) or downward (downscaling). It is natural, on the contrary, for multifractal processes. In fact, to evaluate the effects of the statistics of the small-scale space–time patterns on the longer time scale global statistics, one requires simultaneous simulations of both. Such simulations are, however, now feasible using new multifractal techniques (Wilson *et al.*, 1989; Pecknold *et al.*, 1993; Marsan *et al.*, 1996, 1997), leading to the development of exploratory studies of zooplankton behaviour within multifractal phytoplankton fields (Marguerit *et al.*, 1998) which can be regarded as a new way to investigate the trophodynamics of zooplankton.

Multifractals and, in particular, universal multifractals then appear to be a

potential powerful tool in analysing multiscale space–time variability of any inter-mittent processes and improve on previous studies showing the applicability of non-linear algorithms (Sugihara and May, 1990b; Sugihara *et al.*, 1990; Ascioti *et al.*, 1993; Strutton *et al.*, 1996, 1997a,b) and multifractal analysis (Pascual *et al.*, 1995) to both spatial and temporal planktonic data in several ways. First, the use of universal multifractals provides three fundamental parameters characterizing the organization, or structure, of the whole variability of a given intermittent process, and then allows direct comparisons to be made between biological and physical fields. That is, universal multifractal analysis can be regarded as a way to delineate the relative contributions of the biological and physical processes to the patterns observed, a major issue in marine ecology (Haury *et al.*, 1978; Denman and Powell, 1984; Legendre and Demers, 1984; Mackas *et al.*, 1985; Daly and Smith, 1993). Moreover, even if spectral analysis methods and concepts have played a major role in previous work concerning the identification of the scales of plankton patchiness (Platt and Denman, 1975; Platt, 1978; Fasham, 1978; Harris, 1980), they are largely insufficient to characterize the precise distribution of phyto-plankton biomass, which appears to be essential to provide accurate estimates of the magnitude of related key fluxes such as primary, new and export productions following the extreme sensitivity of numerical modelling even to minor changes in parameter values (Werner *et al.*, 1993). Second, the predictive efficiency of non-linear algorithms, based on interpolations of pre-existing data by a simplex procedure [see, for example, Sugihara and May (1990b) for further details on the nearest-neighbour algorithm] and essentially aimed to distinguish between deter-minist and stochastic components of a given dataset, is poor in comparison with the technique of simulating continuous multifractal cascades (Schertzer and Lovejoy, 1987b; Wilson *et al.*, 1991; Pecknold *et al.*, 1993; Schertzer *et al.*, 1998) which produce fields which are very good approximations—at all scales and inten-sities—of the statistics of the measured field, and determine the probability distri-bution of the field values. Finally, using the concept of first- and second-order multifractal phase transitions, we can characterize the strength of the very rare and violent events present in a given dataset and quantify the range of statistical moments which can be accurately estimated given the finite sample size, respect-ively. In the general background of spatio-temporal intermittency encountered in the ocean (Platt *et al.*, 1989), knowledge of the precise statistics of any intermittent field may avoid the bias introduced by chronic undersampling of an intermittent signal (Bohle-Carbonel, 1992). In that way, universal multifractals may have considerable implications for the design and evaluation of potential sampling schemes in coastal areas as in open ocean, but also to improve estimates of stocks and fluxes associated with heterogeneous distribution of resources and exploiters which will not be robust unless all processes are understood in detail.

These powerful applications of multifractals, which are still under development in a conceptual and modelling way (Marsan *et al.*, 1996, 1997; Schertzer *et al.*, 1998), can then provide new application fields to ecological sciences, opening a large perspective in understanding ecosystem structure, and then could be regarded as a new way to develop individual rather than global approaches in the apprehension of any intermittent pattern and process.

Acknowledgements

We are especially indebted to Dr T.Wyatt for stimulating this paper during our fruitful discussions at the Newton Institute Euroconference 'Modelling the role of zooplankton in marine food chain'. We are also grateful to Drs V.Gentilhomme and F.Lizon for stimulating discussions, and to three anonymous reviewers for helpful suggestions on improving the manuscript. Thanks are also extended to the captain and crew of the N/O 'Côte d'Aquitaine' for their assistance in collecting the data for this paper.

References

Abbott,M.R. and Zion,P.M. (1985) Satellite observations of phytoplankton variability during an upwelling event. *Cont. Shelf Res.*, **4**, 661–680.

Abbott,M.R. and Zion,P.M. (1987) Spatial and temporal variability of phytoplankton pigment of northern California during Coastal Ocean Dynamics Experiment. *J. Geophys. Res.*, **92**, 1745–1755.

Abraham,E.R. (1998) The generation of plankton patchiness by turbulent stirring. *Nature*, **391**, 577–580.

Alcaraz,M., Saiz,E., Marrasé,C. and Vaqué,D. (1988) Effects of turbulence on the development of phytoplankton biomass and copepod populations in marine microcosms. *Mar. Ecol. Prog. Ser.*, **49**, 117–125.

Alldredge,A.L. and Hammer,W.M. (1980) Recurring aggregation of zooplankton by a tidal current. *Estuarine Coastal Mar. Sci.*, **10**, 31–37.

Allen,T.F.H and Hoekstra,T.W. (1991) Role of heterogeneity in scaling of ecological systems under analysis. In Kolasa,J. and Pickett,S.T.A. (eds), *Ecological Heterogeneity*. Springer-Verlag, New York, pp. 47–68.

Allen,T.F.H. and Starr,T.B. (1982) *Hierarchy: Perspectives for Complexity*. Chicago University Press, Chicago.

Anselmet,F., Gagne,Y., Hopfinger,E.J. and Antonia,R.A. (1984) High-order velocity structure functions in turbulent shear flows. *J. Fluid Mech.*, **140**, 63–69.

Ascioti,F.A., Beltrami,E., Carroll,T.O. and Wirick,C. (1993) Is there chaos in plankton dynamics? *J. Plankton Res.*, **15**, 603–617.

Auger,P. and Poggiale,J.-C. (1996) Emergence of population growth models: fast migration and slow growth. *J. Theor. Biol.*, **182**, 99–108.

Baker,M.A. and Gibson,C.H. (1987) Sampling turbulence in the stratified ocean: statistical consequences of strong intermittency. *J. Phys. Oceanogr.*, **17**, 1817–1836.

Batchelor,G.K. and Townsend,A.A. (1949) The nature of turbulent motion at large wavenumbers. *Proc. R. Soc. A*, **199**, 238–250.

Bellehumeur,C., Legendre,P. and Marcotte,D. (1997) Variance and spatial scales in a tropical rain forest: changing the size of sampling units. *Plant Ecol.*, **130**, 89–98.

Belyaev,V.S., Gezentsvey,A.N., Monin,A.S., Ozmidov,R.V. and Paka,V.T. (1975) Spectral characteristics of small-scale fluctuations of hydrophysical fields in the upper layer of the ocean. *J. Phys. Oceanogr.*, **5**, 492–498.

Bennett,A.F. and Denman,K.L. (1985) Phytoplankton patchiness: inferences from particle statistics. *J. Mar. Res.*, **43**, 307–335.

Billen,G. and Lancelot,C. (1988) Modelling benthic nitrogen cycling in coastal ecosystems. In Blackburn,T.H. and Sorensen,J. (eds), *Nitrogen Cycling in Coastal Marine Environments*. Wiley & Sons, New York, pp. 343–378.

Bohle-Carbonel,M. (1992) Pitfalls in sampling, comments on reliability and suggestions for simulation. *Cont. Shelf Res.*, **12**, 3–24.

Brylinski,J.M. and Lagadeuc,Y. (1990) L'interface eau côtière/eau du large dans le Pas-de-Calais (côte française): une zone frontale. *C. R. Acad. Sci. Paris Sér. 2*, **311**, 535–540.

Brylinski,J.-M. *et al.* (1991) Le 'fleuve côtier': un phénomène hydrologique important en Manche orientale. Exemple du Pas-de-Calais. *Oceanol. Acta*, **11**, 197–203.

Cassie,R.M. (1959a) An experimental study of factors inducing aggregation in marine plankton. *N.Z. J. Sci.*, **2**, 339–365.

Cassie,R.M. (1959b) Some correlations in replicate plankton samples. *N.Z. J. Sci.*, **2**, 473–484.

Cassie,R.M. (1960) Factors influencing the distribution pattern of plankton in the mixing zone between oceanic and harbour waters. *N.Z. J. Sci.*, **3**, 26–50.

Cassie,R.M. (1963) Microdistribution in the plankton. *Oceanogr. Mar. Biol. Annu. Rev.*, **1**, 223–252.

Chigirinskaya,Y., Schertzer,D., Lovejoy,S., Lazarev,A. and Ordanovich,A. (1994) Unified multifractal atmospheric dynamics tested in the tropics: part I, horizontal scaling and self criticality. *Nonlin. Processes Geophys.*, **1**, 105–114.

Chigirinskaya,Y., Schertzer,D. and Lovejoy,S. (1997) Scaling gyroscopes cascade: universal multifractal features of 2-D and 3-D turbulence. In Giona,M. and Biardi,G. (eds), *Fractals and Chaos in Chemical Engineering*. World Scientific, Singapore, pp. 371–384.

Corrsin,S. (1951) On the spectrum of isotropic temperature in an isotropic turbulence. *J. Appl. Phys.*, **22**, 469.

Costello,J.H., Strickler,J.R., Marrasé,C., Trager,G., Zeller,R. and Freise,A. (1990) Grazing in a turbulent environment: behavioral response of a calanoid copepod, *Centropages hamatus*. *Proc. Natl Acad. Sci. USA*, **87**, 1648–1652.

Currie,D.J. (1984) Phytoplankton growth and the microscale nutrient patch hypothesis. *J. Plankton Res.*, **6**, 591–599.

Daly,K.L. and Smith,W.O. (1993) Physical-biological interactions influencing marine plankton production. *Annu. Rev. Ecol. Syst.*, **24**, 555–585.

Davis,C.S., Flierl,G.R., Wiebe,P.H. and Franks,P.J.S (1991) Micropatchiness, turbulence and recruitment in plankton. *J. Mar. Res.*, **49**, 109–151.

Demers,S., Lafleur,P.E., Legendre,L. and Trump,C.L. (1979) Short-term covariability of chlorophyll and temperature in the St. Lawrence estuary. *J. Fish. Res. Board Can.*, **36**, 568–573.

Denman,K.L. (1976) Covariability of chlorophyll and temperature in the sea. *Deep-Sea Res.*, **23**, 539–550.

Denman,K.L. and Abbott,M.R. (1988) Time evolution of surface chlorophyll patterns from cross-spectrum analysis of satellite color images. *J. Geophys. Res.*, **93**, 6789–6798.

Denman,K.L. and Platt,T. (1976) The variance spectrum of phytoplankton in a turbulent ocean. *J. Mar. Res.*, **34**, 593–601.

Denman,K.L. and Powell,T.M. (1984) Effects of physical processes on planktonic ecosystems in the coastal ocean. *Oceanogr. Mar. Biol. Annu. Rev.*, **22**, 125–168.

Denman,K.L., Okubo,A. and Platt,T. (1977) The chlorophyll fluctuation spectrum in the sea. *Limnol. Oceanogr.*, **22**, 1033–1038.

Deschamps,P.Y., Frouin,R. and Wald,L. (1981) Satellite determinations of the mesoscale variability of the sea surface temperature. *J. Phys. Oceanogr.*, **11**, 864–870.

Dupont,J.-P., Lafite,R., Huault,M.-F., Lamboy,M., Brylisnki,J.-M. and Guéguéniat,P. (1991) La dynamique des masses d'eau et matière en suspension en Manche orientale. *Oceanol. Acta*, **11**, 177–186.

Elliott,J.A. and Oakey,N.S. (1979) Average microstructure levels and vertical diffusion for phase III, GATE. *Deep-Sea Res.*, **26**, 279–294.

Estrada,M., Alcaraz,M. and Marrasé,C. (1987) Effects of turbulence on the composition of phytoplankton assemblages in marine microcosms. *Mar. Ecol. Prog. Ser.*, **38**, 267–281.

Evans,G.T. (1978) Biological effects of vertical-horizontal interactions. In Steele,J.H. (ed.), *Spatial Patterns in Plankton Communities*. Plenum, New York, pp. 157–179.

Falco,T., Francis,F., Lovejoy,S., Schertzer,D., Kerman,B. and Drinkwater,M. (1996) Universal multifractal scaling of synthetic aperture radar images of sea-ice. *IEEE Trans. Geosci. Remote Sensing*, **34**, 906–914

Fasham,M.J.R. (1978) The statistical and mathematical analysis of plankton patchiness. *Oceanogr. Mar. Biol. Annu. Rev.*, **16**, 43–79.

Fasham,M.J.R. and Pugh,P.R. (1976) Observations on the horizontal coherence of chlorophyll a and temperature. *Deep-Sea Res.*, **23**, 527–538.

Fortier,L., Legendre,L., Cardinal,A. and Trump,C.L. (1978) Variabilité à court terme du phytoplancton de l'estuaire du St-Laurent. *Mar. Biol.*, **46**, 349–354.

Frisch,U., Sulem,P.-L. and Nelkin,M. (1978) A simple dynamical model of intermittent fully developed turbulence. *J. Fluid Mech.*, **87**, 719–724.

Frontier,S. (1987) Application of fractal theory to ecology. In Legendre,P. and Legendre,L. (eds), *Developments in Numerical Ecology*. Springer-Verlag, Berlin, pp. 335–378.

Gentilhomme,V. and Lizon,F. (1998) Seasonal cycle of nitrogen and phytoplankton biomass in a well-mixed coastal system (Eastern English Channel). *Hydrobiologia*, **361**, 191–199.

Gibson,C.H. (1991) Kolmogorov similarity hypotheses for scalar fields: sampling intermittent turbulent mixing in the ocean and galaxy. *Proc. R. Soc. London Ser. A*, **434**, 149–164.

Gower,J.F.R., Denman,K.L. and Holyer,R.J. (1980) Phytoplankton patchiness indicates the fluctu-
ation spectrum of mesoscale oceanic structure. *Nature*, **288**, 157–159.

Granata,T.C. and Dickey,T.D. (1991) The fluid mechanics of copepod feeding in a turbulent flow. A
theoretical approach. *Prog. Oceanogr.*, **26**, 243–261.

Grant,H., Stewart,R. and Moillet,A. (1962) Turbulent spectra from a tidal channel. *J. Fluid Mech.*, **12**,
241–268.

Grassberger,P. (1983) Generalized dimensions of strange attractors. *Phys. Lett.*, **97**, 227–230.

Gregg,M.C. (1980) Microstructure patches in the thermocline. *J. Phys. Oceanogr.*, **10**, 915–943.

Gregg,M.C., Cox,C.S. and Hacker,P.W. (1973) Vertical microstructure measurements in the central
North Pacific. *J. Phys. Oceanogr.*, **3**, 458–469.

Hansen,J., Fung,I., Lacis,A., Rind,D., Lebedeff,S., Ruedy,R., Russel,G. and Stone,P. (1988) Global
climate changes as forecast by the Goddard Institute for Space Studies three dimensional model.
J. Geophys. Res., **93**, 9341–9364.

Hardy,L.R. and Gunther,E.R. (1935) The plankton of the South Georgia whaling grounds and
adjacent waters, 1926–1927. *Discovery Rep.*, **11**, 1–456.

Harris,G.P. (1980) Temporal and spatial scales in phytoplankton ecology. Mechanisms, methods,
models and management. *Can. J. Fish Aquat. Sci.*, **37**, 877–900.

Haury,L.R., McGowan,J.A. and Wiebe,P.H. (1978) Patterns and processes in the time-space scales of
plankton distributions. In Steele,J.H. (ed.), *Spatial Pattern in Plankton Communities*. Plenum, New
York, pp. 277–327.

Hentschel,H.G.E. and Procaccia,I. (1983) The infinite number of generalized dimensions of fractals
and strange attractors. *Physica D*, **8**, 435–444.

Herman,A.W., Sameoto,D.D. and Longhurst,A.R. (1981) Vertical and horizontal distribution
patterns of copepods near the shelf break south of Nova Scotia. *Can. J. Fish. Aquat. Sci.*, **38**,
1065–1076.

Horwood,J.W. (1978) Observations on spatial heterogeneity of surface chlorophyll in one and two
dimensions. *J. Mar. Biol. Assoc. UK*, **58**, 487–502.

Hutchinson,G.E. (1953) The concept of pattern in ecology. *Proc. Natl Acad. Nat. Sci. Philadelphia*,
105, 1–12.

Jarvis,P.G. (1995) Scaling processes and problems. *Plant Cell. Environ.*, **18**, 1079–1089.

Jiménez,J. (1997) Ocean turbulence at millimeter scales. *Sci. Mar.*, **61**, 47–56.

Jiménez,J. and Wray,A.A. (1994) Columnar vortices in isotropic turbulence. *Meccanica*, **29**, 453–464.

Jiménez,J., Wray,A.A., Safman,P.G. and Rogallo,R.S. (1993) The structure of intense vorticity in
isotropic turbulence. *J. Fluid Mech.*, **255**, 65–90.

Jou,D. (1997) Intermittent turbulence: a short introduction. *Sci. Mar.*, **61**, 57–62.

Kamykowski,D. (1974) Possible interactions between phytoplankton and semi-diurnal internal waves.
J. Mar. Res., **32**, 67–89.

Kierstead,H. and Slobodkin,L.B. (1953) The size of water masses containing plankton blooms. *J. Mar.
Res.*, **12**, 141–147.

Kiørboe,T. (1993) Turbulence, phytoplankton cell size and the structure of pelagic food webs. *Adv.
Mar. Biol.*, **29**, 1–72.

Kiørboe,T. (1997) Small-scale turbulence, marine snow formation, and planktivorous feeding. *Sci.
Mar.*, **61**, 141–158.

Kiørboe,T. and MacKenzie,B.R. (1995) Turbulence-enhanced prey encounter rates in larval fish:
effects of spatial scale, larval behaviour and size. *J. Plankton Res.*, **17**, 2319–2331.

Kiørboe,T., Lunsgaard,C., Olesen,M. and Hansen,J.L.S. (1994) Aggregation and sedimentation
processes during a spring phytoplankton bloom: a field experiment to test coagulation theory. *J.
Mar. Res.*, **52**, 297–323.

Kolmogorov,A.N. (1941) The local structure of turbulence in incompressible viscous fluid for very
large Reynolds numbers. *Dokl. Akad. Nauk SSSR*, **30**, 299–303.

Kolmogorov,A.N. (1962) A refinement of previous hypotheses concerning the local structure of
turbulence in viscous incompressible fluid at high Reynolds number. *J. Fluid Mech.*, **13**, 82.

Kraichnan,R.H. (1967) Inertial ranges in two-dimensional turbulence. *Phys. Fluids*, **9**, 1937–1943.

Ladoy,P., Lovejoy,S. and Schertzer,D. (1991) Extreme variability of climatological data: scaling and
intermittency. In Schertzer,D. and Lovejoy,S. (eds), *Non-linear Variability in Geophysics*. Kluwer,
Norwell, pp. 241–250.

Lagadeuc,Y., Brylinski,J.-M. and Aelbrecht,D. (1997) Temporal variability of the vertical stratifi-
cation of a front in a tidal Region of Freshwater Influence (ROFI) system. *J. Mar. Syst.*, **12**, 147–155.

Lavallée,D. (1991) Multifractal techniques: analysis and simulation of turbulent fields. PhD Thesis,
McGill University, Montréal, Canada.

Lavallée,D., Lovejoy,S., Schertzer,D. and Schmitt,F. (1992) On the determination of universal multi-fractal parameters in turbulence. In Moffat,K., Tabor,M. and Zaslavsky,G. (eds), *Topological Aspects of the Dynamics of Fluid and Plasmas*. Kluwer, Boston, pp. 463–478.

Lazarev,A., Schertzer,D., Lovejoy,S. and Chigirinskaya,Y. (1994) Unified multifractal atmospheric dynamics tested in the tropics: Part II, vertical scaling and Generalized Scale Invariance. *Nonlin. Processes Geophys.*, **1**, 115–121.

Legendre,L. and Demers,S. (1984) Towards dynamic biological oceanography and limnology. *Can. J. Fish. Aquat. Sci.*, **41**, 2–19.

Legendre,P. and Fortin,M.J. (1989) Spatial patterns and ecological analysis. *Vegetatio*, **80**, 1055–1067.

Lekan,J.F. and Wilson,R.E. (1978) Spatial variability of phytoplankton biomass in the surface waters of Long Island. *Estuarine Coastal Mar. Sci.*, **6**, 239–251.

Levin,S.A. (1992) The problem of pattern and scale in ecology. *Ecology*, **73**, 1943–1967.

Levin,S.A., Grenfell,B., Hastings,A. and Perelson,A.S. (1997) Mathematical and computational challenges in population biology and ecosystems science. *Science*, **275**, 334–343.

Lovejoy,S. and Schertzer,D. (1985) Generalized scale-invariance in the atmosphere and fractal model of rain. *Water Resour. Res.*, **21**, 1233–1250.

Lovejoy,S. and Schertzer,D. (1990) Multifractals, universality classes and satellite and radar measurements of cloud and rain fields. *J. Geophys. Res.*, **95**, 2021–2034.

Mackas,D.L., Louttit,G.C. and Austin,M.J. (1980) Spatial distribution of zooplankton and phytoplankton in British Columbian coastal waters. *Can. J. Fish Aquat. Sci.*, **37**, 1476–1487.

Mackas,D.L., Denman,K.L. and Abbot,M.R. (1985) Plankton patchiness: biology in the physical vernacular. *Bull. Mar. Sci.*, **37**, 652–674.

MacKenzie,B.R. and Kiørboe,T. (1995) Encounter rates and swimming behavior of pause-travel and cruise larval fish predators in calm and turbulent laboratory environments. *Limnol. Oceanogr.*, **40**, 1278–1289.

MacKenzie,B.R., Miller,T.J., Cyr,S. and Leggett,W.C. (1994) Evidence of a dome-shaped relationship between turbulence and larval fish ingestion rates. *Limnol. Oceanogr.*, **39**, 1790–1799.

Madden,C.J. and Day,J.W. (1992) Induced turbulence in rotating bottles affects phytoplankton productivity measurements in turbid waters. *J. Plankton Res.*, **14**, 1171–1191.

Mandelbrot,B. (1974) Multiplications aléatoires itérées et distributions invariantes par moyenne pondérée aléatoire. *C. R. Acad. Sci. Paris Sér. A*, **278**, 289–292.

Mandelbrot,B. (1977) *Fractals. Form, Chance and Dimension*. Freeman, London.

Mandelbrot,B. (1983) *The Fractal Geometry of Nature*. Freeman, New York.

Marguerit,C., Schertzer,D., Schmitt,F. and Lovejoy,S. (1998) Copepod diffusion within a multifractal phytoplankton field. *J. Mar. Syst.*, **16**, 69–83.

Marquet,P.A., Fortin,M.-J., Pineda,J., Wallin,D.O., Clark,J., Wu,Y., Bollens,J., Jacobi,C.M. and Holt,R.D. (1993) Ecological and evolutionary consequences of patchiness: a marine-terrestrial perspective. In Levin,S.A., Powell,T.M. and Steele,J.H. (eds), *Patch Dynamics*. Springer-Verlag, New York, pp. 277–304.

Marrasé,C., Costello,J.H., Granata,T. and Strickler,J.R. (1990) Grazing in a turbulent environment: energy dissipation, encounter rates, and efficacy of feeding currents in *Centropages hamatus. Proc. Natl Acad. Sci. USA*, **87**, 1653–1657.

Marsan,D., Schertzer,D. and Lovejoy,S. (1996) Causal space-time multifractal processes: predictability and forecasting of rain fields. *J. Geophys. Res.*, **101**, 26333–26346.

Marsan,D., Schertzer,D. and Lovejoy,S. (1997) Predictability of multifractal processes: the case of turbulence. In Giona,M. and Biardi,G. (eds), *Fractals and Chaos in Chemical Engineering*. World Scientific, Singapore, pp. 465–475.

Martin-Jezequel,V. (1983) Facteurs hydrologiques et phytoplancton en Baie de Morlaix (Manche Occidentale). *Hydrobiologia*, **102**, 131–143.

McCave,I.N. (1984) Size-spectra and aggregation of suspended particles in the deep ocean. *Deep-Sea Res.*, **22**, 491–502.

McHardy,I. and Czerny,B. (1987) Fractal X-ray time variability and spectral invariance of the Seyfert galaxy NGC5506. *Nature*, **325**, 696–698.

Meneveau,C. and Sreenivasan,K.R. (1987) Simple multifractal cascade model for fully developed turbulence. *Phys. Rev. Lett.*, **59**, 1424–1427.

Milne,B.T. (1988) Measuring the fractal geometry of landscapes. *Appl. Math. Comp.*, **27**, 67–79.

Mitchell,J.G., Okubo,A. and Fuhrman,J.A. (1985) Microzones surrounding phytoplankton form the basis for a stratified marine microbial ecosystem. *Nature*, **316**, 58–59.

Monin,A.S. and Yaglom,A.M. (1975) *Statistical Fluid Mechanics: Mechanics of Turbulence*. MIT Press, London.

Nihoul,J.C.J. and Djenidi,S. (1991) Hierarchy and scales in marine ecohydrodynamics. *Earth-Science Rev.*, **31**, 255–277.

Novikov,E.A. and Stewart,R. (1964) Intermittency of turbulence and spectrum of fluctuations in energy dissipation. *Izv. Akad. Nauk SSSR Geogr. I Geofiz.*, **3**, 408–412.

Oakey,N.S. (1985) Statistics of mixing parameters in the upper ocean during JASIN Phase 2. *J. Phys. Oceanogr.*, **15**, 1502–1520.

Oakey,N.S. and Elliott,J.A. (1982) Dissipation within the surface mixed layer. *J. Phys. Oceanogr.*, **12**, 171–185.

Obukhov,A.M. (1941) Spectral energy distribution in a turbulent flow. *Dokl. Akad. Nauk SSSR*, **32**, 22–24.

Obukhov,A.M. (1949) Structure of the temperature field in a turbulent flow. *Izv. Akad. Nauk SSSR Geogr. I Geofiz.*, **13**, 55.

Obukhov,A.M. (1962) Some specific features of atmospheric turbulence. *J. Fluid Mech.*, **13**, 77.

Okubo,A. (1978) Horizontal dispersion and critical scales for phytoplankton patches. In Steele,J.H. (ed.), *Spatial Pattern in Plankton Communities*. Plenum Press, New York, pp. 21–42.

Okubo,A. (1980) *Diffusion and Ecological Problems: Mathematical Models*. Springer-Verlag, Berlin.

Okubo,A. (1986) Dynamical aspects of animal grouping: swarms, schools, flocks, and herds. *Adv. Biophys.*, **22**, 1–94.

Olsson,J., Niemczynowicz,J. and Berndtsson,R. (1993) Fractal analysis of high-resolution rainfall time series. *J. Geophys. Res.*, **98**, 265–274.

O'Neill,R.V. (1989) Perspectives in hierarchy and scale. In May,R.M. and Roughgarden,J. (eds), *Ecological Theory*. Princeton University Press, Princeton, pp. 140–156.

O'Neill,R.V., Gardner,R.H., Milne,B.T., Turner,M.G. and Jackson,B. (1991) Heterogeneity and spatial hierarchies. In Kolasa,J. and Pickett,S.T.A. (eds), *Ecological Heterogeneity*. Springer-Verlag, New York, pp. 85–96.

Osborn,T.R. (1978) Measurements of energy dissipation adjacent to an island. *J. Geophys. Res.*, **83**, 2939–2957.

Osborn,T.R. and Lueck,R.G. (1985a) Turbulence measurement from a towed body. *J. Atmos. Oceanic Technol.*, **2**, 517–527.

Osborn,T.R. and Lueck,R.G. (1985b) Turbulence measurement with a submarine. *J. Phys. Oceanogr.*, **15**, 1502–1520.

Owen,R.W. (1981) Fronts and eddies in the sea: mechanisms, interactions and biological effects. In Longhurst,A.R. (ed.), *Analysis of Marine Ecosystems*. Academic Press, London, pp. 197–233.

Paffenhöfer,G.-A. (1994) Variability due to feeding activity of individual copepods. *J. Plankton Res.*, **16**, 617–626.

Parisi,G. and Frisch,U. (1985) A multifractal model of intermittency. In Ghil,M., Benzi,R. and Parisi,G. (eds), *Turbulence and Predictability in Geophysical Fluid Dynamics and Climate Dynamics*. North Holland, Amsterdam, pp. 84–88.

Pascual,M., Ascioti,F.A. and Caswell,H. (1995) Intermittency in the plankton: a multifractal analysis of zooplankton biomass variability. *J. Plankton Res.*, **17**, 1209–1232.

Pecknold,S., Lovejoy,S., Shertzer,D., Hooge,C. and Malouin,J.F. (1993) The simulation of universal multifractals. In Perdang,J.M. and Lejeune,A. (eds), *Cellular Automata: Prospects in Astrophysical Applications*. World Scientific, Singapore, pp. 228–267.

Peters,F. and Gross,T. (1994) Increased grazing rates of microplankton in response to small-scale turbulence. *Mar. Ecol. Prog. Ser.*, **115**, 299–307.

Pingree,R.D., Mardell,G.T., Reid,P.C. and John,A.W.G. (1986) The influence of tidal mixing on the timing of the spring phytoplankton development in the southern of the North Sea, the English Channel and the northern Armorican Shelf. In Bowman,J., Yentsch,M. and Peterson,W.T. (eds), *Tidal Mixing and Plankton Dynamics*. Springer-Verlag, New York, pp. 164–192.

Platt,T. (1972) Local phytoplankton abundance and turbulence. *Deep-Sea Res.*, **19**, 183–187.

Platt,T. (1978) Spectral analysis of spatial structure in phytoplankton populations. In Steele,J.H. (ed.), *Spatial Pattern in Plankton Communities*. Plenum, New York, pp. 73–84.

Platt,T. and Denman,K.L. (1975) Spectral analysis in ecology. *Annu. Rev. Ecol. Syst.*, **6**, 189–210.

Platt,T., Dickie,L.M. and Trites,R.W. (1970) Spatial heterogeneity of phytoplankton in a near-shore environment. *J. Fish. Res. Board Can.*, **27**, 1453–1473.

Platt,T., Harrison,W.G., Lewis,M.R., Li,W.K.W., Sathyendranath,S., Smith,R.E. and Vezina,A.F. (1989) Biological production of the oceans: the case for a consensus. *Mar. Ecol. Prog. Ser.*, **52**, 77–88.

Poggiale,J.-C. (1998a) From behavioural to population level: growth and competition. *Math. Comput. Model.*, **27**, 41–49.

Poggiale,J.-C. (1998b) Predator-prey models in heterogeneous environments: emergence of functional response. *Math. Comput. Model.*, **27**, 63–71.

Powell,T.M. and Okubo,A. (1994) Turbulence, diffusion and patchiness in the sea. *Philos. Trans. R. Soc. London Ser. B*, **343**, 11–18.

Powell,T.M., Richerson,P.J., Dillon,T.M., Agee,B.A., Dozier,B.J., Godden,D.A. and Myrup,L.O. (1975) Spatial scales of current speed and phytoplankton biomass fluctuations in Lake Tahoe. *Science*, **189**, 1088–1089.

Prairie,Y.T. and Duarte,C.M. (1996) Weak density-dependence and short-term perturbations as determinants of phytoplankton temporal dynamics. *Ecoscience*, **3**, 451–460.

Quisthoudt,C. (1987) Production primaire phytoplanctonique dans le détroit du Pas-de-Calais (France): variations spatiales et annuelles au large du cap Griz-Nez. *C. R. Acad. Sci. Paris*, **304**, 245–250.

Raby,D., Lagadeuc,Y., Dobson,J.J. and Mingelbier,M. (1994) Relationship between feeding and vertical distribution of bivalves larvae in stratified and mixed waters. *Mar. Ecol. Prog. Ser.*, **103**, 275–284.

Richardson,L.F. (1922) *Weather Prediction by Numerical Processes*. Cambridge University Press, Cambridge.

Riebesell,U. (1991a) Particle aggregation during a diatom bloom. I. Physical aspects. *Mar. Ecol. Prog. Ser.*, **69**, 273–280.

Riebesell,U. (1991b) Particle aggregation during a diatom bloom. II. Biological aspects. *Mar. Ecol. Prog. Ser.*, **69**, 281–291.

Riley,G.A. (1976) A model of plankton patchiness. *Limnol. Oceanogr.*, **21**, 873–880.

Rothschild,B.J. and Osborn,T.R. (1988) Small-scale turbulence and plankton contact rates. *J. Plankton Res.*, **10**, 465–474.

Salomon,J.-C. and Breton,M. (1993) An atlas of long-term currents in the Channel. *Oceanol. Acta*, **16**, 439–448.

Scherrer,B. (1984) *Biostatistiques*. Morin, Boucherville.

Schertzer,D. and Lovejoy,S. (1983) The dimension and intermittency of atmospheric dynamics. In Launder,B. (ed.), *Turbulent Shear Flows 4*. Springer-Verlag, Karlsruhe, pp. 7–33.

Schertzer,D. and Lovejoy,S. (1985) Generalised scale invariance in turbulent phenomena. *Physico-Chem. Hydrodyn. J.*, **6**, 623–635.

Schertzer,D. and Lovejoy,S. (1987a) Physical modeling and analysis of rain and clouds by anisotropic scaling multiplicative processes. *J. Geophys. Res.*, **92**, 96–99.

Schertzer,D. and Lovejoy,S. (1987b) Physically based rain and cloud modeling by anisotropic multiplicative turbulent cascades. *J. Geophys. Res.*, **92**, 9693–9714.

Schertzer,D. and Lovejoy,S. (1989) Nonlinear variability in geophysics: multifractal analysis and simulation. In Pietronero,L. (ed.), *Fractals: Physical Origin and Consequences*. Plenum, New York, pp. 49–79.

Schertzer,D. and Lovejoy,S. (1992) Hard and soft multifractal processes. *Physica A*, **185**, 187–194.

Schertzer,D. and Lovejoy,S. (1997) Universal multifractals do exist! *J. Appl. Meteorol.*, **36**, 1296–1303.

Schertzer,D., Lovejoy,S., Lavallée,D. and Schmitt,F. (1991) Universal hard multifractal turbulence, theory and observations. In Sagdeev,R.Z., Frisch,U., Hussain,F., Moiseev,S.S. and Erokhin,N.S. (eds), *Nonlinear Dynamics of Structures*. World Scientific, Singapore, pp. 213–235.

Schertzer,D., Lovejoy,S. and Schmitt,F. (1995) Structures in turbulence and multifractal universality. In Meneguzzi,M., Pouquet,A. and Sulem,P.L. (eds), *Small-scale Structure in 3D Fluid and MHD Turbulence*. Springer-Verlag, New York, pp. 137–144.

Schertzer,D., Lovejoy,S., Schmitt,F., Chigirinskya,Y. and Marsan,D. (1998) Multifractal cascade dynamics and turbulent intermittency. *Fractals*, **5**, 427–471.

Schmitt,F., Lavallée,D., Shertzer,D. and Lovejoy,S. (1992a) Empirical determination of universal multifractal exponents in turbulent velocity fields. *Phys. Rev. Lett.*, **68**, 305–308.

Schmitt,F., Lavallée,D., Lovejoy,S., Schertzer,D. and Hooge,C. (1992b) Estimations directes des indices de multifractals universels dans le champ de vent et de température. *C. R. Acad. Sci. Paris Sér. II*, **314**, 749–754.

Schmitt,F., Schertzer,D., Lovejoy,S. and Brunet,Y. (1993) Estimation of universal multifractal indices for atmospheric turbulent velocity fields. *Fractals*, **1**, 568–575.

Schmitt,F., Schertzer,D., Lovejoy,S. and Brunet,Y. (1994) Empirical study of multifractal phase transitions in atmospheric turbulence. *Nonlin. Processes Geophys.*, **1**, 95–104.

Seuront,L. (1997) Distribution inhomogène multiéchelle de la biomasse phytoplanctonique en milieu turbulent. *J. Rech. Océanogr.*, **22**, 9–16.

Seuront,L. and Lagadeuc,Y. (1997) Characterisation of space-time variability in stratified and mixed

coastal waters (Baie des Chaleurs, Québec, Canada): application of fractal theory. *Mar. Ecol. Prog. Ser.*, **259**, 81–95.

Seuront,L. and Lagadeuc,Y. (1998) Spatio-temporal structure of tidally mixed coastal waters: variability and heterogeneity. *J. Plankton Res.*, **20**, 1387–1401.

Seuront,L., Schmitt,F., Lagadeuc,Y., Schertzer,D., Lovejoy,S. and Frontier,S. (1996a) Multifractal analysis of phytoplankton biomass and temperature in the ocean. *Geophys. Res. Lett.*, **23**, 3591–3594.

Seuront,L., Schmitt,F., Lagadeuc,Y., Schertzer,D. and Lovejoy,S. (1996b) Multifractal intermittency of Eulerian and Lagrangian turbulence of ocean temperature and plankton fields. *Nonlin. Processes Geophys.*, **3**, 236–246.

Sharples,J. and Tett,P. (1994) Modelling the effect of physical variability on the midwater chlorophyll maximum. *J. Mar. Res.*, **52**, 219–238.

Skellam,J.G. (1951) Random dispersal in theoretical populations. *Biometrika*, **38**, 196–218.

Stavn,R.H. (1971) The horizontal-vertical distribution hypothesis: Langmuir circulations and Daphnia distributions. *Limnol. Oceanogr.*, **16**, 453–466.

Steele,J.H. (1974) Spatial heterogeneity and population stability. *Nature*, **248**, 83.

Steele,J.H. (1976) Patchiness. In Cushing,D.H. and Walsh,J.J. (eds), *Ecology of the Sea*. Blackwell, London, pp. 98–115.

Steele,J.H. (1978) Some comments on plankton patches. In Steele,J.H. (ed.), *Spatial Patterns in Plankton Communities*. Plenum, New York, pp. 1–20.

Steele,J.H. (1988) Scale selection for biodynamics theories. In Steele,J.H. (ed.), *Spatial Patterns in Plankton Communities*. Plenum, New York, pp. 513–526.

Steele,J.H. (1991) Can ecological theory cross the land-sea boundary? *J. Theor. Biol.*, **153**, 425–436.

Steele,J.H. and Henderson,E.W. (1977) Plankton patches in the Northern North Sea. In Steele,J.H. (ed.), *Fisheries Mathematics*, Academic Press, London, pp. 1–19.

Steele,J.H. and Henderson,E.W. (1992) A simple model for plankton patchiness. *J. Plankton Res.*, **14**, 1397–1403.

Stommel,H. (1949) Trajectories of small bodies sinking slowly through convection cells. *J. Mar. Res.*, **8**, 24–49.

Stommel,H. (1963) Varieties of oceanographic experience. *Science*, **139**, 572–576.

Strutton,P.G., Mitchell,J.G. and Parslow,J.S. (1996) Non-linear analysis of chlorophyll a transects as a method of quantifying spatial structure. *J. Plankton Res.*, **18**, 1717–1726.

Strutton,P.G., Mitchell,J.G. and Parslow,J.S. (1997a) Using non-linear analysis to compare the spatial structure of chlorophyll with passive tracers. *J. Plankton Res.*, **19**, 1553–1564.

Strutton,P.G., Mitchell,J.G., Parslow,J.S. and Greene,R.M. (1997b) Phytoplankton patchiness: quantifying the biological contribution using Fast Repetition Rate Fluorometry. *J. Plankton Res.*, **19**, 1265–1274.

Sugihara,G. and May,R.M. (1990a) Applications of fractals in ecology. *Trends Ecol. Evol.*, **5**, 79–86.

Sugihara,G. and May,R.M. (1990b) Nonlinear forecasting as a way of distinguishing chaos from measurement error in time series. *Nature*, **344**, 734–741.

Sugihara,G., Grenfell,B. and May,R.M. (1990) Distinguishing error from chaos in ecological time series. *Philos. Trans. R. Soc. London Ser. B*, **330**, 235–251.

Sundby,S. and Fossum,P. (1990) Feeding conditions of Arcto-Norwegian cod larvae compared with the Rothschild–Osborn theory on small-scale turbulence and plankton contact rates. *J. Plankton Res.*, **12**, 1153–1162.

Taylor,G.I. (1938) The spectrum of turbulence. *Proc. R. Soc. London Ser. A*, **164**, 476–490.

Teissier,Y., Lovejoy,S. and Schertzer,D. (1993a) Universal multifractals: theory and observations of rain and clouds. *J. Appl. Meteorol.*, **32**, 223–250.

Teissier,Y., Lovejoy,S., Schertzer,D., Lavallée,D. and Kerman,B. (1993b) Universal multifractal indices for the ocean surface at far red wavelengths. *Geophys. Res. Lett.*, **20**, 1167–1170.

Thomas,W.H. and Gibson,C.H. (1990) Effects of small-scale turbulence on microalgae. *J. Appl. Phycol.*, **2**, 71–77.

Verhagen,J.H.G. (1994) Modeling phytoplankton patchiness under the influence of wind-driven currents in lakes. *Limnol. Oceanogr.*, **39**, 1551–1565.

Waite,A. and Harrison,P.J. (1992) Role of sinking and ascent during sexual reproduction in the marine diatom *Ditylum brightwelli*. *Mar. Ecol. Prog. Ser.*, **87**, 113–122.

Wasburn,L. and Gibson,C.H. (1984) Measurements of oceanic temperature microstructure using a small conductivity sensor. *J. Geophys. Res.*, **87**, 4230–4240.

Werner,F.E., Page,F.H., Lynch,D.R., Loder,J.W., Lough,R.G., Perry,R.I., Greenberg,D.A. and Sinclair,M.M. (1993) Influences of mean advection and simple behavior on the distribution of cod and haddock early life stages on Georges Bank. *Fish. Oceanogr.*, **2**, 43–64.

Wiegand,R.C. and Pond,S. (1979) Fluctuations of chlorophyll and related physical parameters in British Columbia coastal waters. *J. Fish. Res. Board Can.*, **36**, 113–121.

Wiens,J.A. (1989) Spatial scaling in ecology. *Funct. Ecol.*, **3**, 385–397.

Wilson,J., Lovejoy,S. and Schertzer,D. (1989) Physically based cloud modelling by scaling multiplicative processes. In Shertzer,D. and Lovejoy,S. (eds), *Scaling, Fractals and Non-linear Variability in Geophysics*. Kluwer, Dordrecht, pp. 185–208.

Wroblewski,J.S. and O'Brien,J.J. (1976) A spatial model of phytoplankton patchiness. *Mar. Biol.*, **35**, 161–175.

Yamazaki,H. (1993) Lagrangian study of planktonic organisms: perspectives. *Bull. Mar. Sci.*, **53**, 265–278.

Yamazaki,H. and Haury,L. (1993) A new Lagrangian model to study animal aggregation. *Ecol. Model.*, **69**, 99–111.

Yamazaki,H. and Kamykowski,D. (1991) The vertical trajectories of motile phytoplankton in a wind-mixed water column. *Deep-Sea Res.*, **38**, 219–241.

Zakardjian,B. and Prieur,L. (1994) A numerical study of primary production related to vertical turbulent diffusion with special reference to vertical motions of the phytoplankton cells in nutrient and light fields. *J. Mar. Syst.*, **5**, 267–295.

Zar,J.H. (1996) *Biostatistical Analysis*. Prentice-Hall International, Englewood Cliffs.